

Boletín Geológico, 46, 23–49, 2020
[https://doi.org/10.32685/0120-1425/
boletingeo.46.2020.534](https://doi.org/10.32685/0120-1425/boletingeo.46.2020.534)



This work is distributed under the Creative Commons Attribution 4.0 License.

Received: June 26, 2019

Accepted: April 13, 2020

Published online: June 30, 2020

Contribution of bedding to the petrophysical characterization of naturally fractured reservoirs: Example of the Matachines fields, Upper Magdalena Valley (*Valle Superior del Magdalena – VSM*) Colombia

Contribución de la estratificación en la caracterización petrofísica de reservorios naturalmente fracturados: ejemplo de los campos Matachines (VSM, Colombia)

Eduardo A. Rossello¹ and José Luis Saavedra²

¹ CONICET (National Scientific and Technical Research Council) – IGEBAs (Institute of Basic, Applied and Environmental Geosciences of Buenos Aires) – UBA (University of Buenos Aires) – FCEN (Faculty of Exact and Natural Sciences). Buenos Aires, Argentina

² Hocol Petroleum Limited, Bogotá, Colombia

Email: ea_rossello@yahoo.com.ar

ABSTRACT

The Matachines field, located in the Girardot subbasin, Upper Magdalena Valley (*Valle Superior del Magdalena – VSM*) basin, has a morphology characterized by antiforms arranged along a N–S axis. These antiforms involve multiphase tectono-sedimentary sequences with half-graben geometries associated with Mesozoic sequences reactivated by at least three Andean phases. Bedding surfaces are mechanically active planes that contribute to the flexural slip that is generated by the folding of multilithologic sequences. In the Matachines field, the bedding planes help to improve the petrophysical characteristics of the reservoirs by incorporating a significant number of discontinuities, which complement the fluid connectivity. Thus, the subhorizontal planes are linked to subvertical fractures preferentially arranged in the ENE–WSW direction, generated by horizontal compressive stress. In particular, these effects are magnified on the western flank and hinge zone of the anticline structure, where they contribute greatly to the connectivity of the production wells. In naturally fractured reservoirs, the correct 4D technical and economic evaluation of the quality and arrangement of discontinuities is essential to determine their actual contribution to improving the petrophysical

properties of such reservoirs. Accordingly, many methods often used to study wells from core samples or images identify, along with different types of fractures, the presence of bedding surfaces, although they evaluate them separately, so they overlook petrophysical factors that affect the porosity and permeability of the wells. The present study discusses the genetic and morphological aspects of bedding surfaces that enhance the petrophysical potential of reservoirs, which usually have limited primary values of permeability and porosity, to meet the economic expectations of specific resources in hydrocarbon exploration and/or production activities.

Keywords: Petrophysics, unconventional reservoirs, hydraulic fracturing, Matachines field, VSM, Colombia.

RESUMEN

Los campos Matachines, localizados en la subcuenca de Girardot (cuenca del valle superior del Magdalena), presentan una morfología antiformal con su eje dispuesto en rumbo submeridional que involucra secuencias tectosedimentarias multifásicas en las que pueden reconocerse geometrías de hemigraben asociadas con las secuencias mesozoicas que han sido reactivadas por al menos tres fases andinas. Las superficies de estratificación son planos mecánicamente activos contribuyentes de los flexodeslizamientos que genera el plegamiento de secuencias multilitológicas. En los campos Matachines, la estratificación contribuye a mejorar las características petrofísicas de sus reservorios al incorporar una importante participación de discontinuidades que complementan la conectividad de los fluidos. Así, desde sus posiciones subhorizontales se vincula con los planos de fracturas subverticales dispuestos preferencialmente en dirección ENE-WSW, generados por los esfuerzos compresionales horizontales. En particular, estos efectos se magnifican sobre el flanco occidental y charnelar de la estructura anticlinal, donde exhiben una mayor participación en la conectividad de los pozos productivos. En los reservorios considerados naturalmente fracturados, la correcta evaluación técnico-económica 4D de la calidad y disposición de las discontinuidades es fundamental para determinar las mejoras petrofísicas que determinan. En este sentido, muchas metodologías habitualmente aplicadas en el estudio de pozos a partir de núcleos o imágenes reconocen, además de distintos tipos de fracturas, la presencia de superficies de estratificación. Sin embargo, se las evalúa separadamente, lo que no incide estadísticamente en las consideraciones petrofísicas que contribuyen a evaluar su porosidad y permeabilidad. Se discuten los aspectos genéticos y morfológicos de las superficies de estratificación que contribuyen a aumentar la potencialidad petrofísica de los reservorios, cuyos valores primarios de permeabilidad y porosidad suelen ser limitados, para sostener expectativas económicas satisfactorias de ciertos recursos en actividades de exploración o producción de hidrocarburos.

Palabras clave: petrofísica, reservorios no convencionales, fracturación, campo Matachines, VSM, Colombia.

1. INTRODUCTION

In naturally fractured hydrocarbon reservoirs, the correct 4D technical and economic evaluation of the quality and arrangement of fractures is essential to determine their actual contribution to improving the petrophysical properties of such reservoirs. Many petrophysical methods that are often used to study wells from core samples of images (Aguilera and Aguilera, 2004; Bratton et al., 2006;

Serra, 2008) identify and quantify the presence of bedding surfaces, but they evaluate them in separate statistical analyses and not within the petrophysical model. Thus, by analyzing them separately from discordant fractures, they are overlooked in geo-economics considerations of their reservoirs.

Naturally fractured reservoirs often present a production paradox because their initially high productivity tends to decline rapidly. Many are also responsible

for early gas or water penetration. However, they include some of the largest and most productive reservoirs, explaining the growing industry efforts to learn more about them and to more accurately model them.

The Matachines field (03°49' N–74°53' W) is located in the Girardot subbasin, within the Upper Magdalena Valley (*Valle Superior del Magdalena* – VSM) basin, similarly to the Purificación, Chenche, and Guando oilfields (Figure 1). The structure of these oilfields is generally characterized by tight and faulted anticlines and by wide synclines with an axis that runs roughly NNE–SSW, related to west-vergence thrust faults that are linked to the uplift of the Eastern Cordillera of Columbia (Campbell and Burgl, 1965; Corrigan, 1967; Anderson, 1972; Butler and Schamel, 1988; Cooper et al., 1995; Barrero et al., 2007 and Higuera, 2012, among many others).

In the present study, the structural aspects that contribute to creating the genetic and morphological characteristics of the bedding surfaces underlying the petrophysical potential of the Matachines field reservoirs are discussed. We focus on sectors where the primary permeability and

porosity values are usually too low to meet economic expectations in hydrocarbon exploration or production activities. These analyses and interpretations may be used to evaluate oilfields with similar characteristics that will be subjected to exploration and/or production.

2. METHODS

A multidisciplinary study was conducted to correctly evaluate deformation features associated with fractures. This study included the analysis of well core or borehole samples, borehole image logs, and a field study aimed at characterizing the physical attributes of the fractures, such as their geometry, direction, aperture, length, and spacing, to classify them into sets. All discontinuity surfaces analyzed in the present study ranged in size from meters to decimeters.

The seismic data were analyzed on a WorkStation mounted on the Petrel platform to spatiotemporally characterize the deformations by horizon flattening of sequences related to the study area, thereby establishing a relative

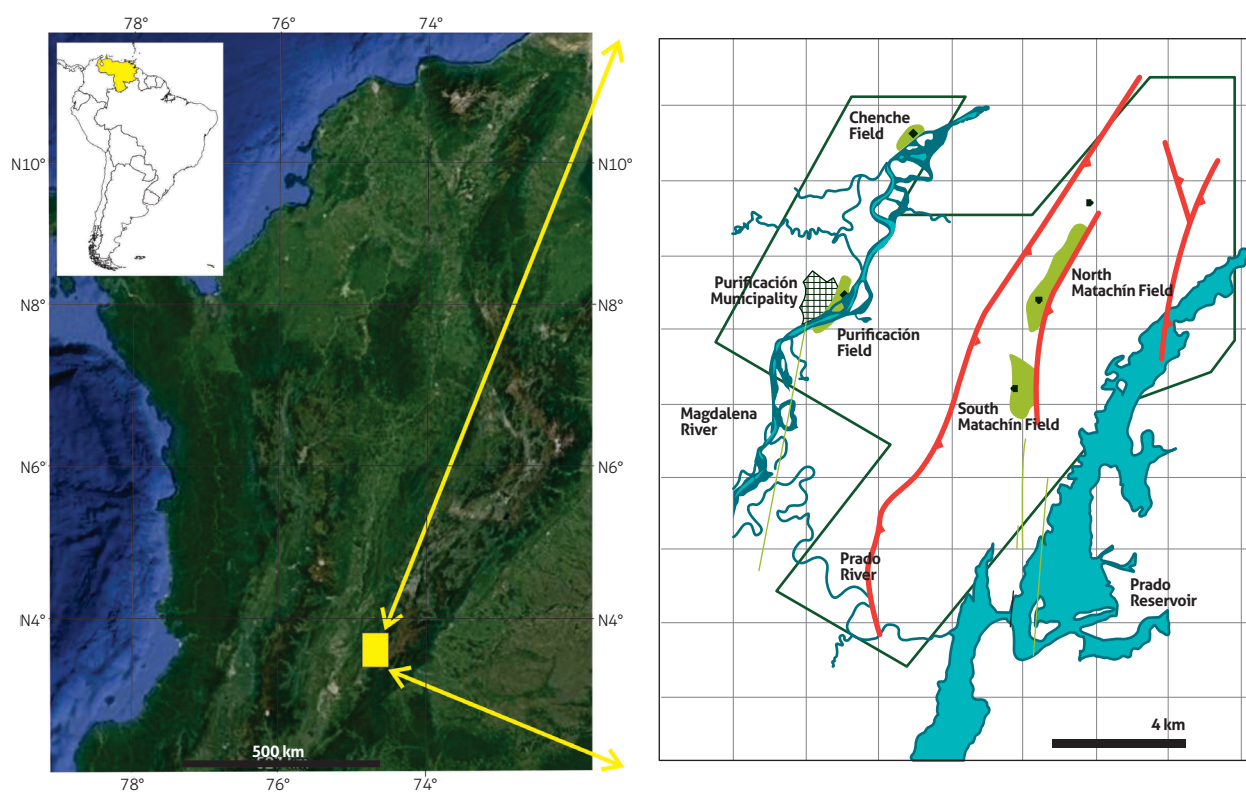


Figure 1. Location of the Matachines field in the VSM

criterion to recognize structures before and after the units that make up the oil system of the Matachines field.

Core samples were analyzed considering the above, as extensively described by Nelson (1985), Aguilera (2001), and by Kubik and Lowry (1993), among others. The available core samples were tentatively arranged and spatially oriented according to strike and dip data of the corresponding wells. The structures were qualitatively and quantitatively analyzed, organoleptically identifying some of their mineralogical components, using magnifying glasses in more detailed cases.

Ultrasonic borehole images are electronic records of well images that provide information on the slope and azimuth of layers and fractures. These data were tabulated, analyzed, and grouped as a function of slope and azimuth (Ekstrom et al., 1987) using the algorithm proposed by Fisher (Fisher et al., 1987) because, in general, this method yields data that are quasi-normally distributed and requires the mean direction and a concentration parameter for input. The main direction data of the fractures and microfaults were plotted on stereograms (lower hemisphere) to assess the vertical configuration of the fractures in the reservoirs.

This analysis generated a set of characteristic attributes of each fracture pattern, which were tabulated in data-processing software to quantify their occurrence percentages, particularly focusing on the identification of friction surfaces (slickensides), to determine the direction of the movements in the discontinuity surfaces.

Data were collected from two study areas in a structural position analogous to the field to analyze fractures in outcrops, primarily measuring representative fracture sets by microtectonics to contrast them with the structures observed in ultrasonic borehole images and core samples.

3. GEOLOGICAL FRAMEWORK OF THE MATACHINES FIELD

From the standpoint of regional tectonics, VSM is bordered to the west, in the Cordillera Central (Central Andes), by the Calarma thrust fault system with eastward vergence, and to the east, in the Cordillera Oriental (East Andes), by faults with opposite vergence, such as the Magdalena fault system (Schamel, 1991; Cooper et al., 1995; Toro et al., 2004).

Morphostructural features derived from surface and subsoil data indicate the multiphase evolution of the Matachines field, which is like that of other regions of VSM (Figure 2). The main stages of its history, based on our own data and on interpretations compiled from the abundant related bibliography, are listed below (*e.g.*, Irving, 1975; Kroonenberg and Diederix, 1982; Mojica and Franco, 1990; Bayona et al., 1994; Villamil et al., 1999; Sarmiento, 2001; Gómez et al., 2003; Sarmiento and Rangel, 2004; Montes et al., 2005; Mora et al., 2010).

3.1 First pre-Andean extensional stage

The tectonic history of the VSM basin started in the Triassic–Jurassic as a retroarc depocenter, which may have been controlled, at least partly, by pre-existing Paleozoic anisotropies (De Freitas, 2001). Half-graben geometries are fairly well preserved, albeit usually modified by the reactivation of at least three Andean phases, which are described below. Then, during the Cretaceous–Early Tertiary, the VSM basin continued as an intracratonic depocenter with the marine sequences of seals of the Caballos Formation (Duarte et al., 2018), generating the hydrocarbons of the Villeta and Guadalupe Groups, resulting in the seals of the Guaduas Formation (Higuera, 2012). Marine transgression and basin subsidence continued during the late Albian until the Santonian, with the VSM basin reaching its maximum extension during the Turonian–Coniacian period (limestones of the La Luna Formation), with the deposition of sediments very rich in organic matter, such as limestones from the Tetuán Formation, pelites from the Bambucá Formation, and pelites and limestones from the Luna Formation, from oldest to youngest (Buitrago, 1994).

Subsequent basin shallowing led to the development of the shallow marine detrital facies of the Guadalupe Group, which is the main producer of several fields (Matachines, Purificación, and Guando) in the Girardot subbasin and of the Monserrate Formation in the Neiva subbasin (Barrero et al., 2007). Marine regression during the Late Cretaceous, with coastline progradation, caused the deposition of fluvio-deltaic sediments of the Guaduas Formation (Late Maastrichtian?–Paleocene), but uplifts during the early-to-middle Eocene eroded these sediments in the highest sections of the basin (Cooper et al., 1995).

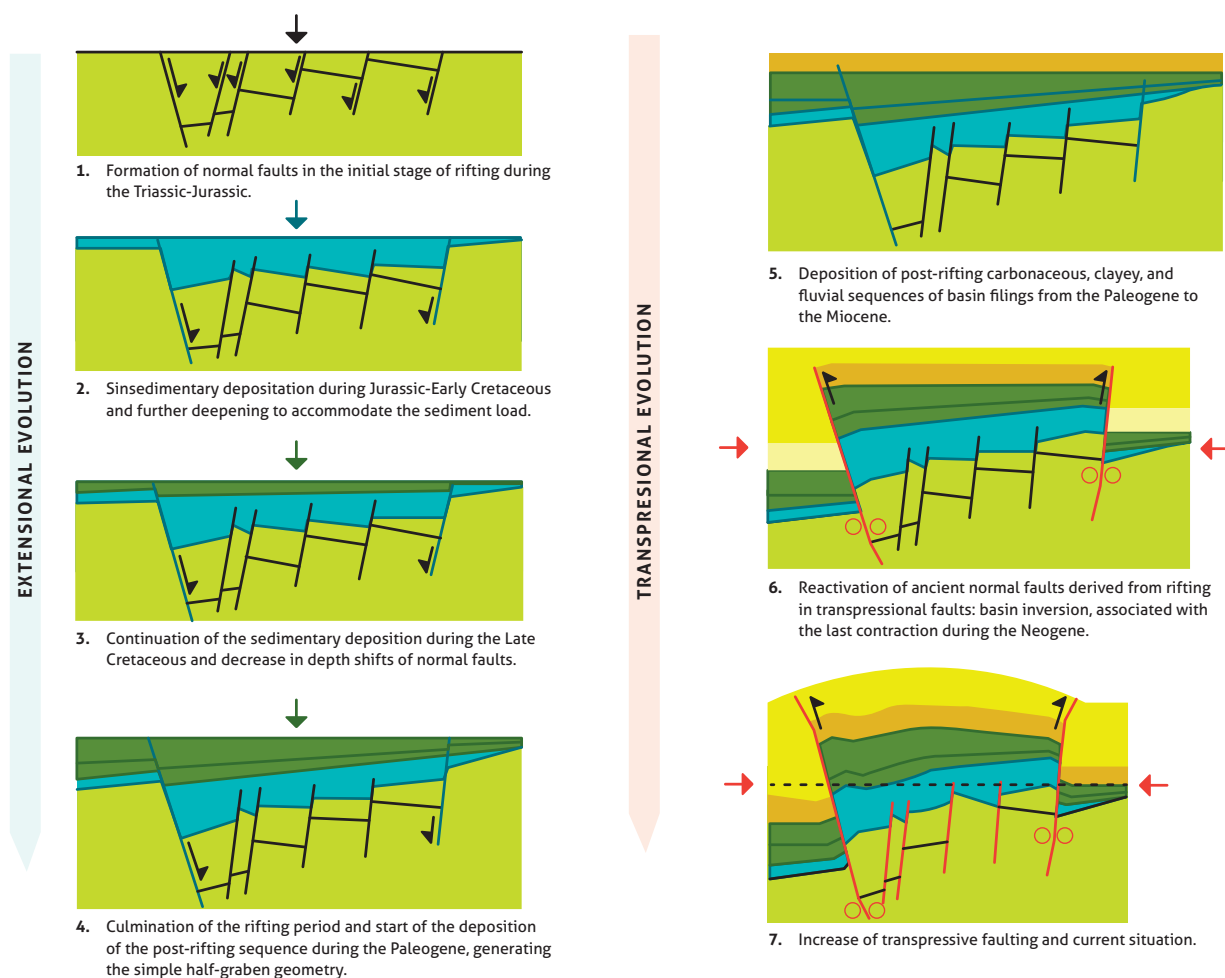


Figure 2. Idealized scheme of the structural evolution of VSM

3.2 Peruvian phase (first stage of compressional inversion)

The Peruvian phase (Cobbold et al., 2007), or the “Mochica event” (De Freitas et al., 2006), has been in general overlooked in Colombia, despite its comprehensive characterization in the rest of the Andes (Pindell and Tabbutt, 1995). In VSM, the Peruvian phase overlaps with the Albian–Cenomanian, as discussed by Jaimes and De Freitas et al. (2006), based on observations by Van der Wiel (1991) in the Garzón massif. De Freitas et al. (2006) recognized evidence of this phase in the Balcón region, where they observed half-graben geometries with clear mild inversions, which occurred during the Late Albian–Cenomanian, as shown by thinning and overlap of pelites of the Bambucá Formation. The NNW–ESE direction of the faulting suggests that compression primarily occurs

in the WSW–ENE direction, which would transpressio-nally reactivate the Jurassic faulting in the ENE direction. Thus, they suggested that an early uplift of the Balcón area during this phase may have positively affected the oil system by generating secondary porosity in the Caballos Formation and by controlling subsequent deformations and migration patterns.

3.3 Incaic phase (second stage of compressional inversion)

The Incaic phase of Andean orogeny started during the early Eocene (for further details, please refer to Cobbold et al., 2007), with the increase in the speed of convergence between the Nazca plate and the South American plate, a determinant of crustal shortening structures expressed by thrust faults involving the basement, especially in the

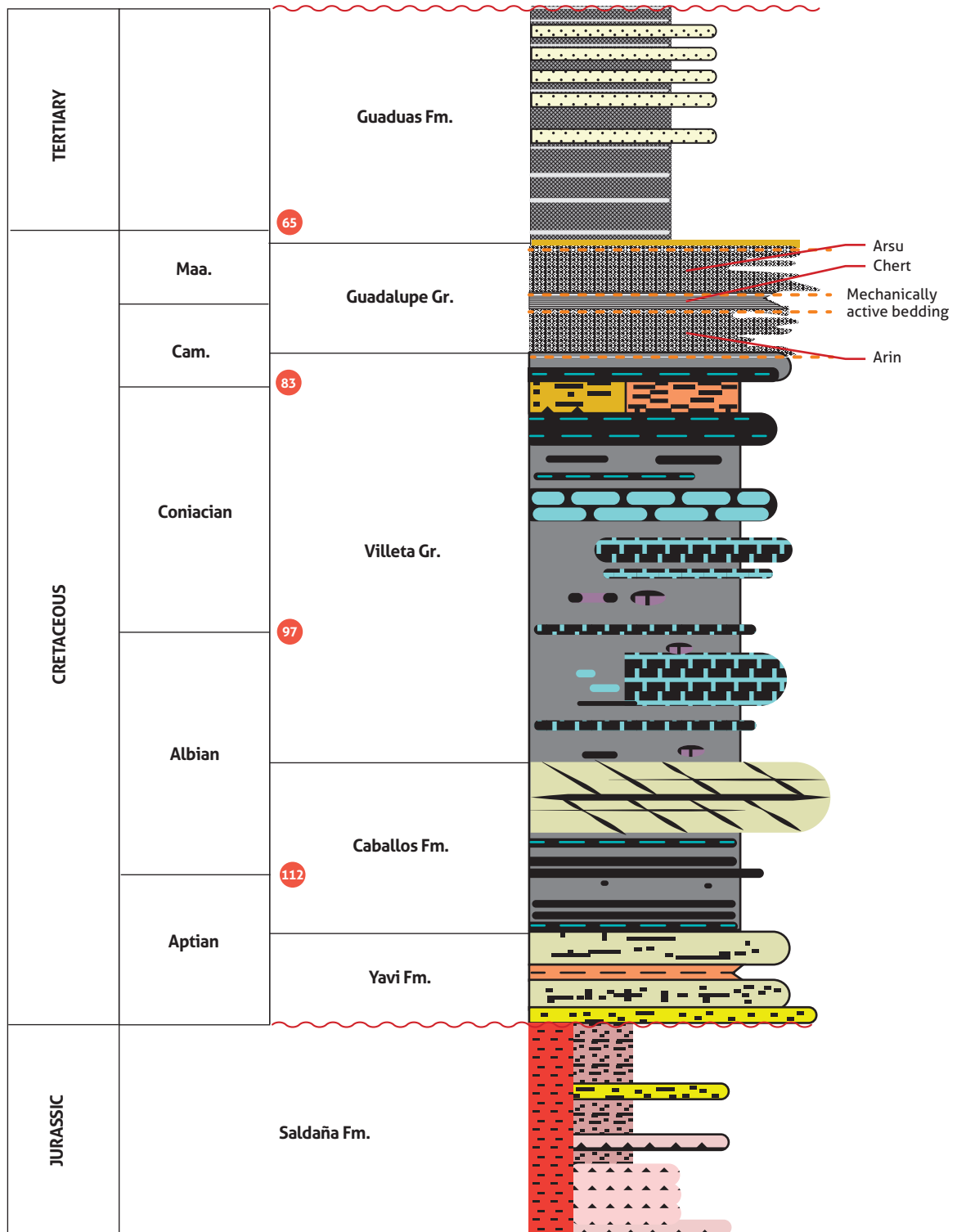


Figure 3. Generalized stratigraphic column of VSM, related to the oil system of the Matachines field

areas neighboring or on the western and eastern margins of the Cordillera Central. The continental sediments of the Gualanday Group were deposited from the late Eocene until the late Oligocene. The Incaic phase, the “Early Andean event” (De Freitas et al., 2006), is identified in the Balcón area by Cenomanian horizon flattening (top of the Bambucá Formation) in seismic interpretation, where the angular discordance postdates the most intense deformation pulse of the area. This event is widely distributed in VSM and has been partly obliterated by the most modern Andean tectonic phases. Despite generating controversy, the age of this discordance is most often attributed to the Middle Eocene (*e.g.*, Schamel, 1991; Cooper et al., 1995; George et al., 1997). However, De Freitas et al. (2006), in line with Buitrago (1994), consider that this discordance is younger, with an Oligocene age in the Neiva subbasin because it is immediately superimposed by the Barzalosa Formation (late Oligocene to early Miocene) by the basal section of the Honda Group, attributed to the middle Miocene (Guerrero, 2002). The configuration produced during this phase persists until the late Miocene, when the oil generation peaks, and is thus a key controlling factor of hydrocarbon entrapment (Higuera, 2012).

3.4 Quechua phase (last stage of compressional-transpressional inversion)

Between the late Miocene and the present Quechua phase of Andean orogeny (Cobbold et al., 2007), the deformation and uplift of the Cordillera Oriental led to another compression period, with new thrust faults with westward vergence, which correspond to the Boquerón fault system, and subsequent deposition of continental sediments of the Honda Formation. The Quechua phase, or the “Andean” event of De Freitas et al. (2006), caused the main uplifts of the region, including those of the Cordillera Oriental, which through thrust faults such as the Garzón fault superimpose these mountain ranges on VSM and produce the exhumation of Jurassic rocks exceeding 8,000 feet. In the Neiva region, an ENE–WSW compression is suggested by numerous folds, whose axes are arranged perpendicularly, preferentially in the WSW direction. This deformation succeeded the deposits of the Honda Formation, dated to the middle Miocene (Guerrero, 2002). Similarly, a discordance is observed at the base of

the Gigante (or Mesa) Formation, which was presumably formed between the late Miocene and the Pliocene and which is gently uplifted in the eastern flank of the basin (De Freitas and Vallejo, 2000). During the Pliocene, strike-slip faults developed along the NW–SE direction, involving the basement and displacing the axes of the folds and of the main faults, due to differential movements of large blocks. Later, from the middle Tertiary, the VSM basin became a marginal foreland basin with continental deposits of the Gualanday Group and Barzalosa Formation, and finally, from the late Tertiary to the present, it became an intermountain basin with the deposits of the Honda Formation (Barrero et al., 2007).

The Neiva and Girardot subbasins of VSM are structural depocenters of the late Cenozoic staggered between the Columbian Cordillera Central and Oriental, which contain three main depositional sequences up to 9,000 m thick on a Paleozoic crystalline basement, which are summarized as follows: 1) Triassic to Jurassic nonmarine siliciclastic rocks and underlying carbonate sequences; 2) Middle Cretaceous to Paleogene marine to nonmarine clastic and carbonate sequences; and 3) a Neogene potent nonmarine molasse-like sequence. According to Beltrán and Gallo (1979), to Buitrago (1994) and to Higuera (2012), the sandstones of the Guadalupe Group (Campanian-Maastrichtian) were deposited in a marine environment from the shallow shelf through the continental shelves to marine-influenced coastal shelves (Figure 3).

The Guadalupe formation contains the main productive reservoirs with petrophysical characteristics, according to observations of outcrops and core samples available in and collected from the various exploration and production wells. These make it possible to differentiate an Upper Guadalupe or “Arup” alloformation (upper sandstones) and a Lower Guadalupe or “Arlo” alloformation (lower sandstones), separate from the Middle Guadalupe or “chert” alloformation (Figure 4).

The pelites of the Villeta Group (late Albian to Santonian) are the main hydrocarbon-generating rocks, and the oil extracted from the fields may come from generation areas located in the nearest synclines or from the vertically deepest areas of production structures (Barrero et al., 2007; Higuera, 2012).

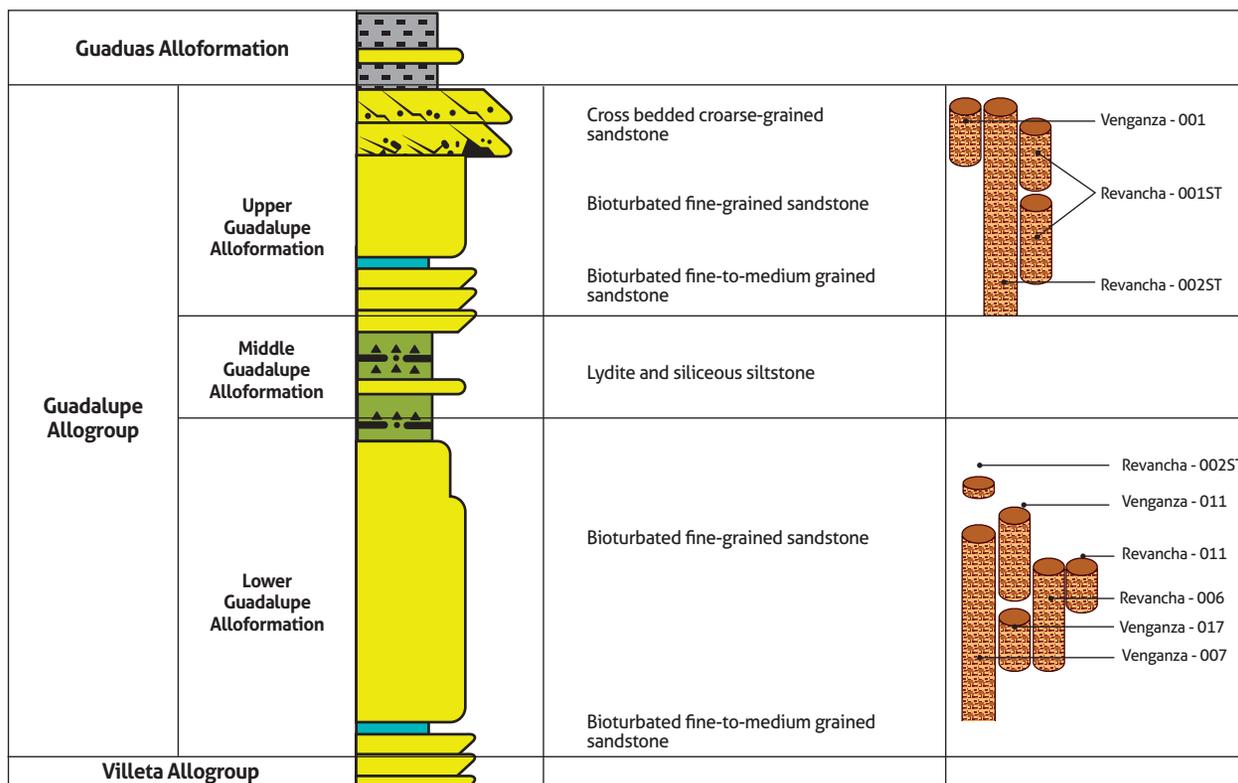


Figure 4. Petrophysical characteristics of the Guadalupe Allogroup, based on outcrop data and core samples

4. STRUCTURAL OBSERVATIONS OF THE MATACHINES FIELD

The Matachines field is located immediately west of the southern end of the Prado syncline and west of the prominent reliefs of the Guadalupe Formation (Figure 5).

The main hydrocarbon production zone is associated with horizons of the Guadalupe Formation, consisting of structural traps with effective closures located in the hinge area of an asymmetric anticline (with a flatter western flank and a steeper eastern flank) and with a N-S axis, gently dipping towards both ends. The Venganza fault is arranged immediately above the hydrocarbon production zone, differentially bisecting the upper flanks, so that the upper ranges of the Guadalupe Formation (Arup) are partly absent in the eastern section (Figure 6).

A plan view of the Matachines field shows the asymmetric anticline that generates this field, with a steeper eastern flank than western flank. The South Matachines Field is not a simple structural continuation of the North Matachines Field and is related to the gradual change

in subsidence of the Venganza fault plane, to the southward tilt of the reservoir layers and to the presence of structural imbrications (Saavedra, 2013). The westward change in direction of the South Matachines Field in relation to the North Matachines Field results from the action of a structural transfer in the sinistral transverse direction (intra-Matachines transverse zone) to the main fold structure (Figure 7).

In a sublatitudinal section, a differentially eroded asymmetric fold affected by compressional faulting is identified, showing a two-scale model based on the South Matachines Field (Figure 8).

Secondary reverse faults increase the structural complexity of the area of interest in such a way that the Guadalupe Formation is repeated in structural units, as found in well REV 09; thus, other reservoir horizons most likely exist in the area. Based on the interpretation of the well logs, the Guadalupe Formation would have been affected by the second detachment and saturated with oil in the REV 01 well. From a morphological standpoint, the hydrocarbon-producing horizons of the Guadalupe For-

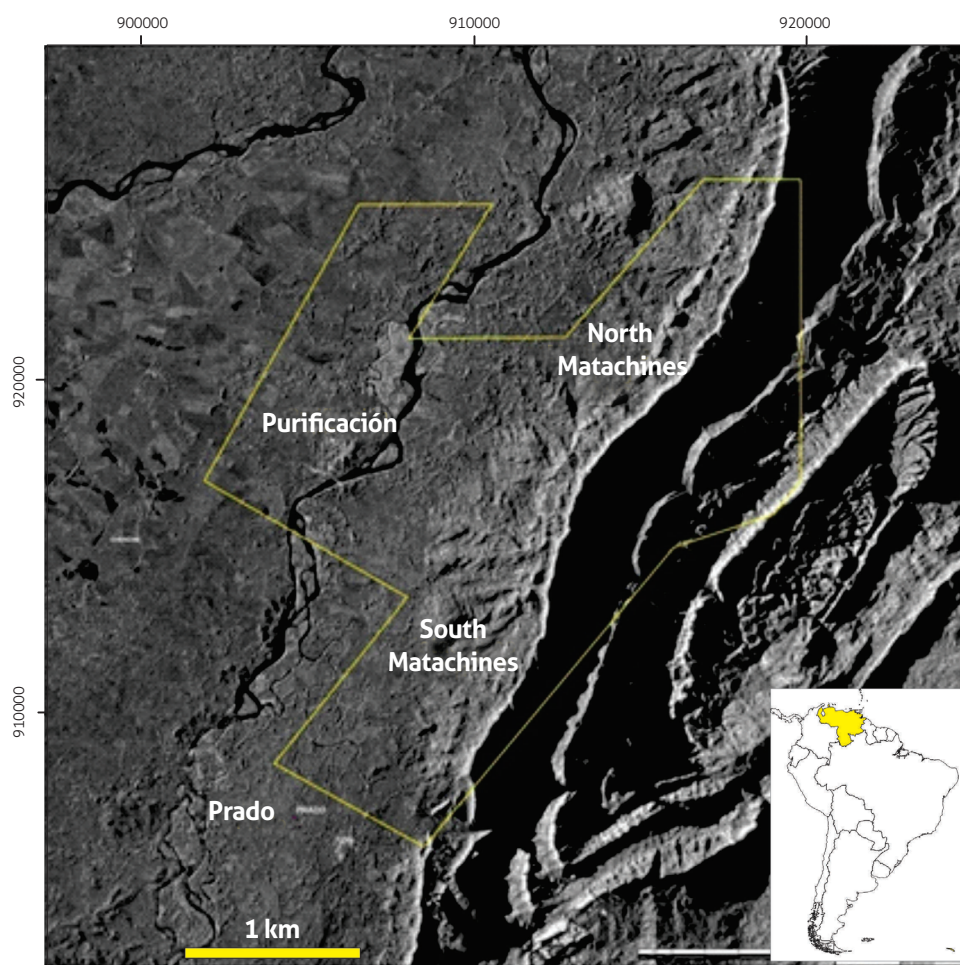


Figure 5. Digital topographic map of the South and North Matachines Field and Purificación, located between the Prado syncline and the Magdalena River

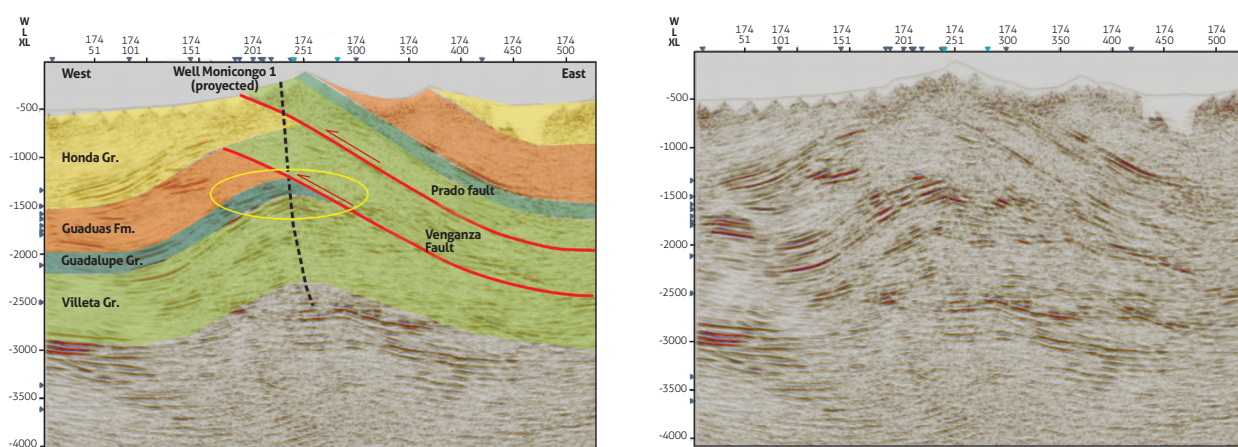


Figure 6. Characteristic sublatitudinal seismic cross-section of a Matachines field. Extracted from a project in WorkStation in which the main structural characteristics were represented (for the location, see Figure 4)

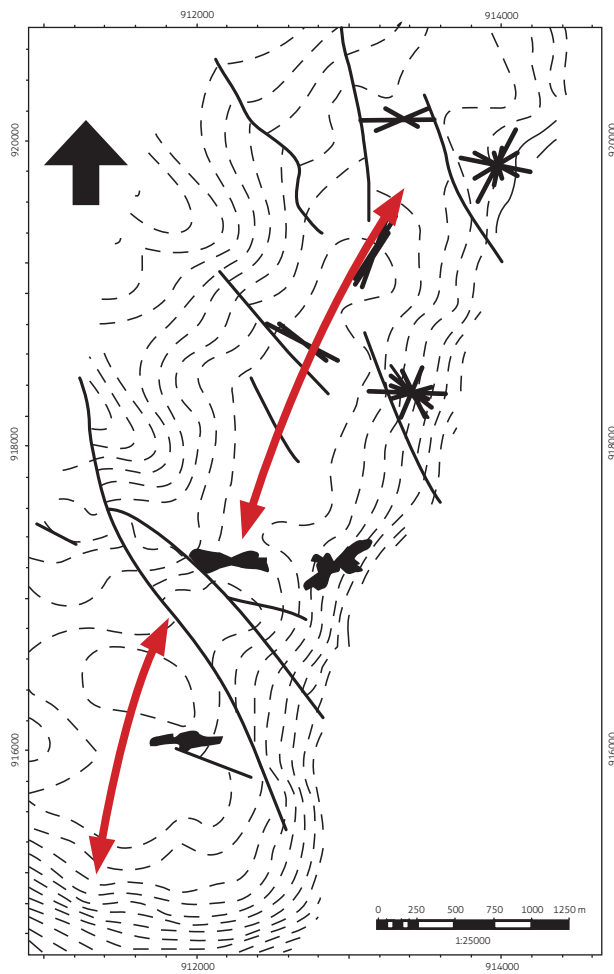


Figure 7. Plan-view map of the Venganza fault structure showing the distribution of the fractures based on well log data

mation are discontinuous due to the truncation of the Paleocene discordance. These horizons are intact in the western flank, but only the lower Guadalupe Formation (Arlo) horizons are preserved in the eastern flank.

According to the available GPS data on the tectonic movement (Tremkamp et al., 2002; Acosta et al., 2004), the current horizontal maximum principal stress field is arranged sublatitudinally due to the sublatitudinal convergence between the Nazca and South America plates, albeit with variable rates and directions. The maximum horizontal principal effort is oblique to the Caribbean margin, indicating a dextral transpressional component,

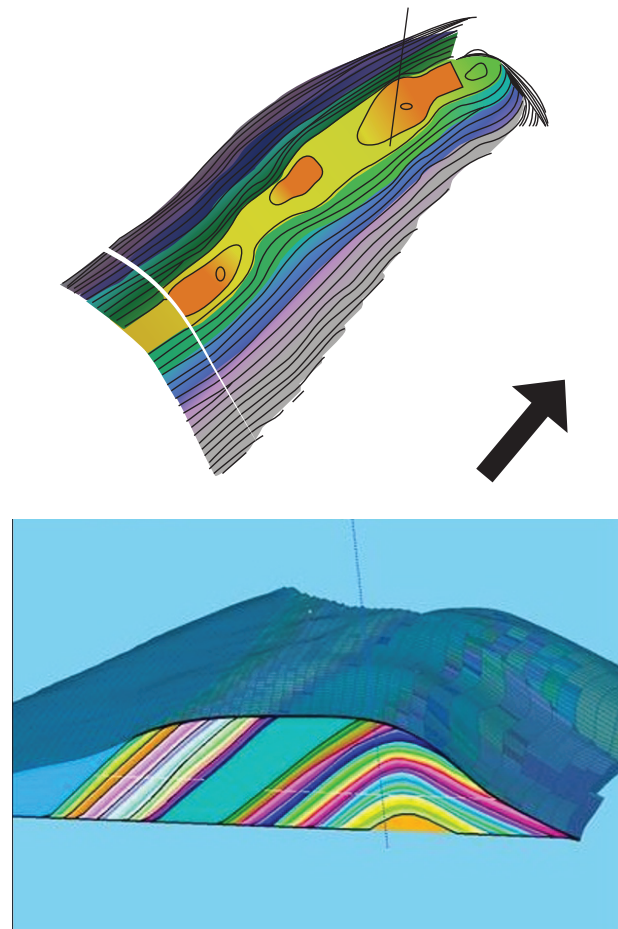


Figure 8. Hydrocarbon-producing horizons of the Guadalupe Formation partly truncated by the Paleocene discordance of the basement of the Gualanday Formation and intersected by the thrust fault Revancha (blue surface), which overlaps Mesozoic sequences (example of the VEN 7 well)

highlighting dextral strike-slip components in the faults of the NE-SW quadrant and sinistral strike-slip components in the faults of the NW-SE quadrant.

The overlap pattern of the Honda Formation across the discordance and the direction of its layers indicates a clockwise rotation of the compressive stress, now oriented in the NW-SE direction, which would have caused an uplift of approximately 2,500 feet from an intra-Honda Formation reference level (De Freitas et al., 2006). Fault kinematics data collected south of the Balcón area corroborate this direction of transportation (Blanco and de Freitas, 2003).

5. NATURALLY FRACTURED RESERVOIRS

Based on the fracture evidence, the Guadalupe Formation reservoirs can be characterized as “naturally fractured” reservoirs because their timely and persistent fractures may also help to accumulate hydrocarbons. Formation micro-imaging (FMI) and petrographic analyses of limestones of the Villeta Group in the Monicongo-1 well suggest the presence of a good reservoir. In addition, despite the low density of these fractures, their aperture (considering Aguilera, 2001) suffices to reach a permeability higher than 1,000 mD.

As the Guadalupe Formation does not adequately outcrop in the Matachines field sectors, to acquire microtectonic data, surveys were conducted near the access road to the Prado dam, where the wide and clear artificial cut made it possible to perform semiquantitative observations (Figure 9).

The outcrops show fractures that, depending on the granulometric characteristics of the horizons of the affected Guadalupe Formation, develop differential spacing and magnitude patterns (Figure 10 and Figure 11).

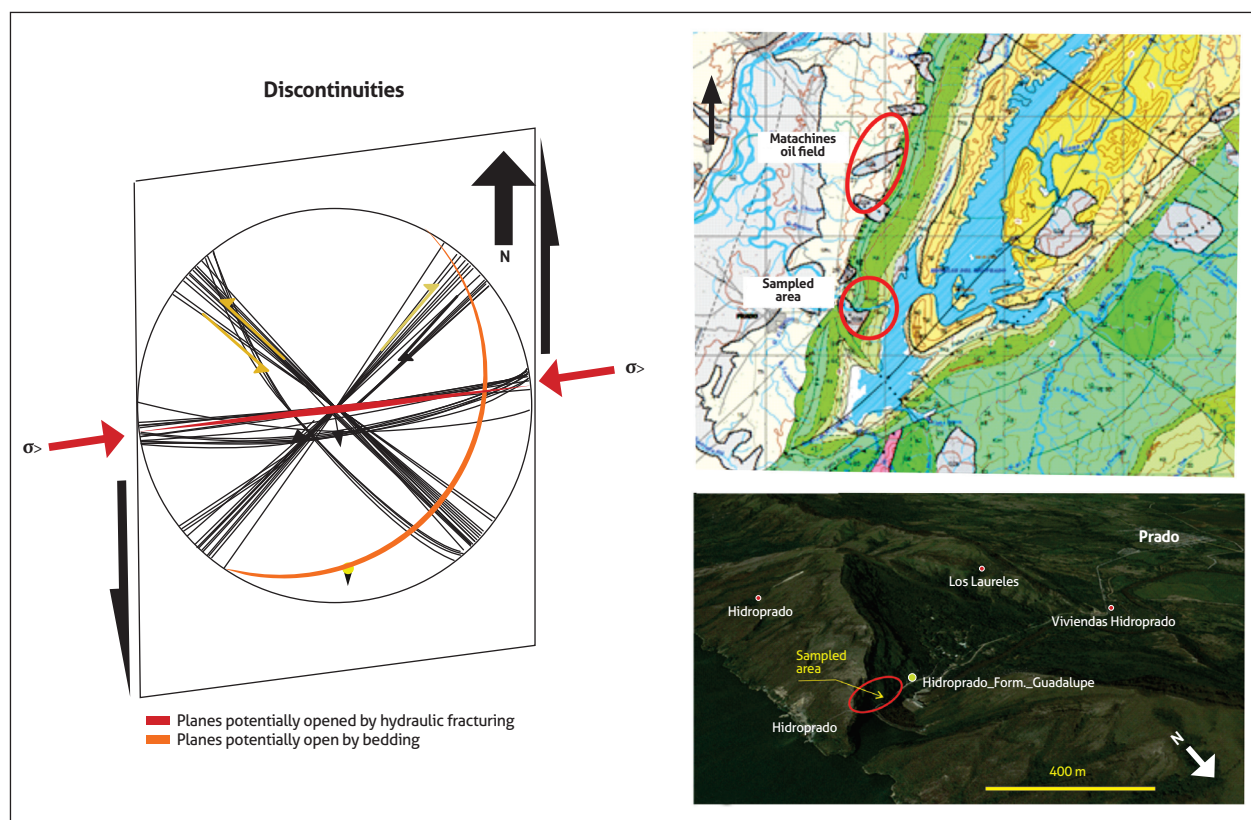


Figure 9. Diagram of fractures surveyed on the access road to the Prado dam. Interpretation of planes potentially opened by hydraulic fracturing and by bedding on the access road to the Prado dam correlated with the Matachines fields (geological map retrieved from Cossio et al., 1995)

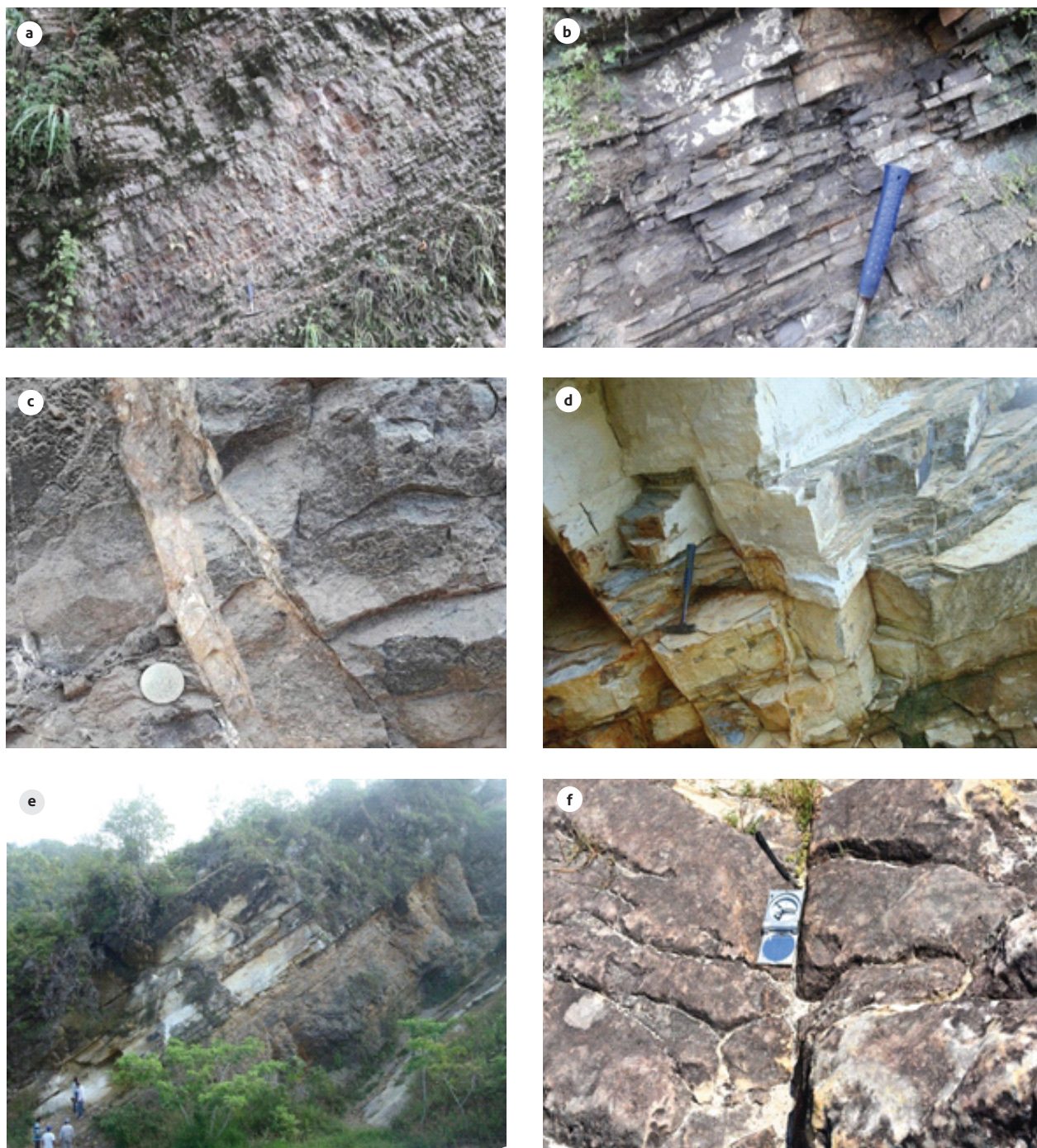


Figure 10. Photographs of the Guadalupe Formation. a) Detail of pelite sequences on the access road to the Prado dam. b) Detail of sequences of fine sandstones on the access road to the Prado dam. c) Detail of subvertical fractures filled with carbonates, arranged sublatitudinally. d) Detail of discordant and concordant fractures with sandstone bedding (chert) on the access roadcut to the Prado dam. e) View of the sequences tilted eastward on the road between Melgar and Icononzo. f) Detail of E-W fractures in the Guadalupe Formation (Arup), on the top of the mountain range of the Tres Mesetas camp

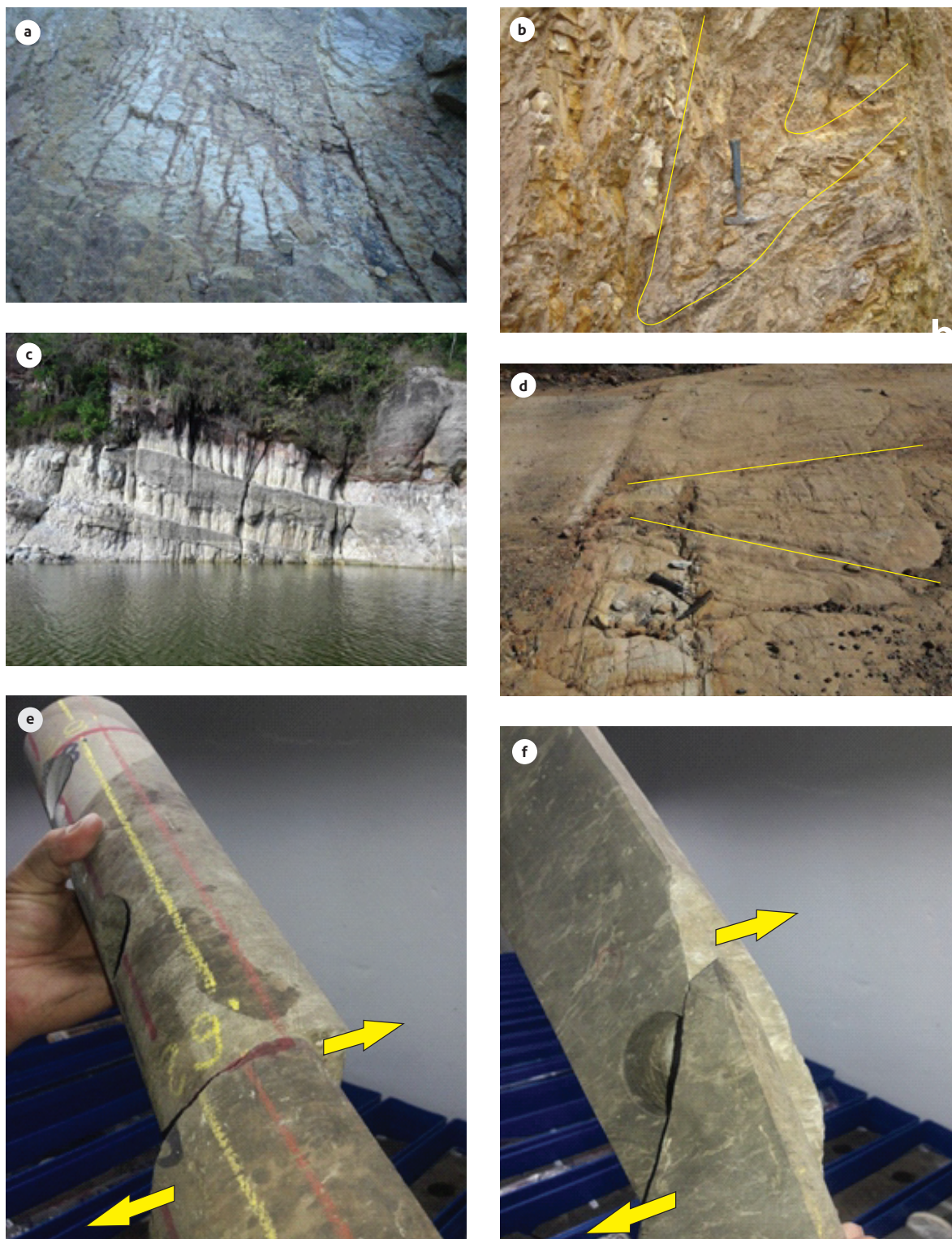


Figure 11. Photographs: a) fractures in sandstone strata of the Guadalupe Formation on a quarry stone road between Guando and Icononzo. b) Folds in pelite horizons of the Guadalupe Formation on the pass of the Melgar-Icononzo route. c) Fractures located in Tertiary sandstone horizons in the Prado reservoir. d) Fractures of the Caballos Formation, on the road to Tomogó. e) Dextral strike-slip fault in a REV1-ST1 well core sample; a 38° plunge in the 107° azimuth direction in layers of the Guadalupe Formation, with bedding at a 34°-35° angle in the 274-284° azimuth direction, approximately located by 3D analysis. f) Subvertical Dextral strike-slip fault with a N-S axis in a REV1-ST1 well core sample, approximately located by 3D analysis

6. RESULTS

Bedding surfaces are mechanically active planes that can considerably enhance the flexural slip produced by the folding of multilithologic sequences (Jamison, 1997). In the Matachines field, bedding also improves the petrophysical characteristics of its reservoirs by incorporating a significant number of discontinuities, thereby complementing fluid connectivity from subhorizontal positions through planes of subvertical fractures generated by the horizontal compressional stresses, which are preferentially arranged in the ENE–WSW direction. In particular, these effects are magnified on the western flank of the anticline structure and to a large extent participate in the connectivity of production wells (Figure 12).

The images of the available wells of fine sand horizons, in light-gray colors, with rhythmic laminations with bioturbations, show microfractures concurrent with

postsedimentary structures, which were used by subsequent faults. Thus, for example, one of the main characteristics of fractures interpreted in the VEN-40 well is that they are conductive, preferentially with an axis along the E–W direction and rarely in the NE–SW direction. The highest fracture density, accounting for 67% of the total data (722), ranges from 0 to 1.6 fractures per foot, distributed between hydrocarbon-producing horizons (Arlo-2, Arlo-3, and Arlo-4). In the other 23% of the data, fracture density ranges from 2 to 3 fractures per foot. The microfractures have planes with E–W and NNE–SSW directions, on average, and are preferentially located on an upper chert (from 6,970 to 7,021' MD), at a 60° angle (to the axis of the well) and with angles of inclination ranging from 70° to 90°. The main characteristic of the fractures interpreted in the VEN-15 well is that they are conductive, with an axis preferentially in the E–W direction and with rare NE–SW fractures (Figure 13).

Spatial distribution of potentially open planes that may contribute to the petrophysical characteristics of the reservoirs

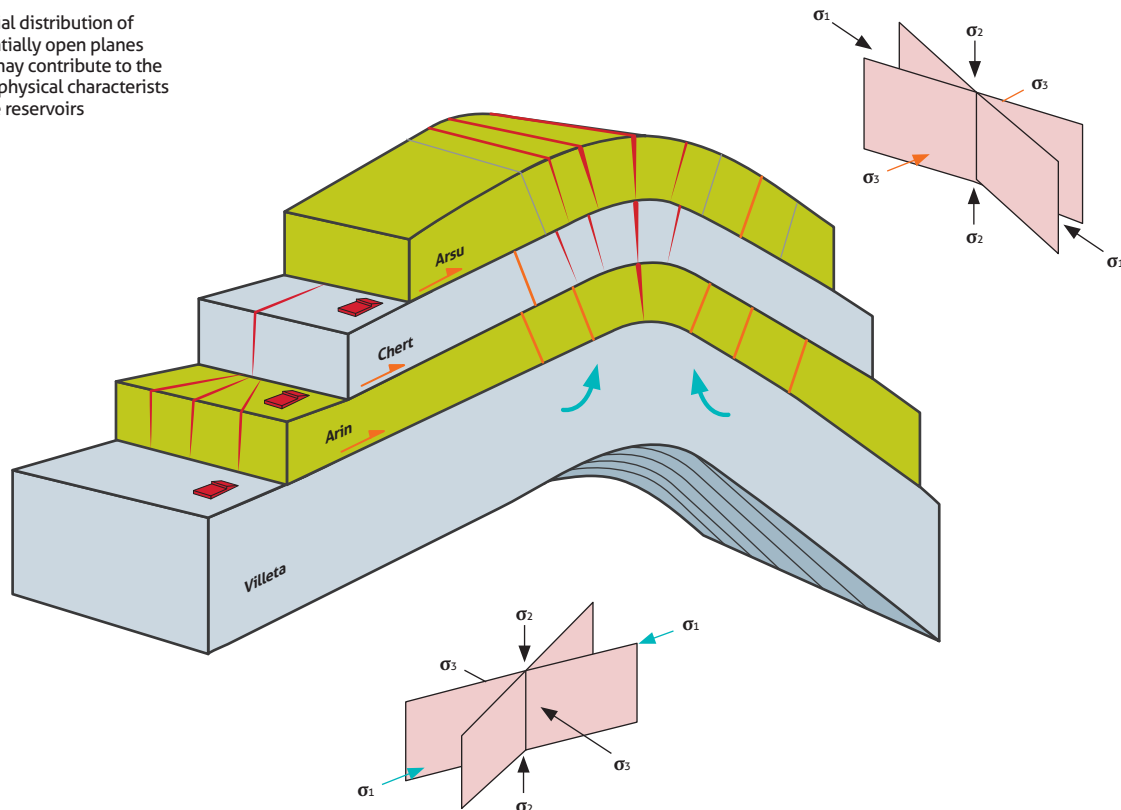


Figure 12. Idealized diagram of the planes potentially responsible for improving the petrophysical quality of unconventional reservoirs

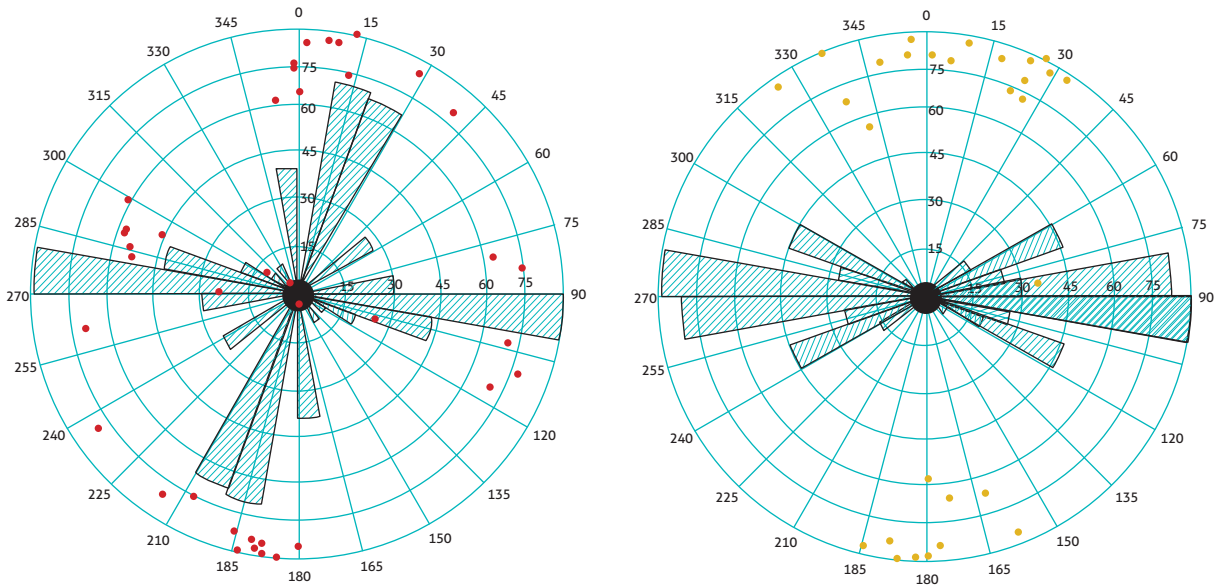
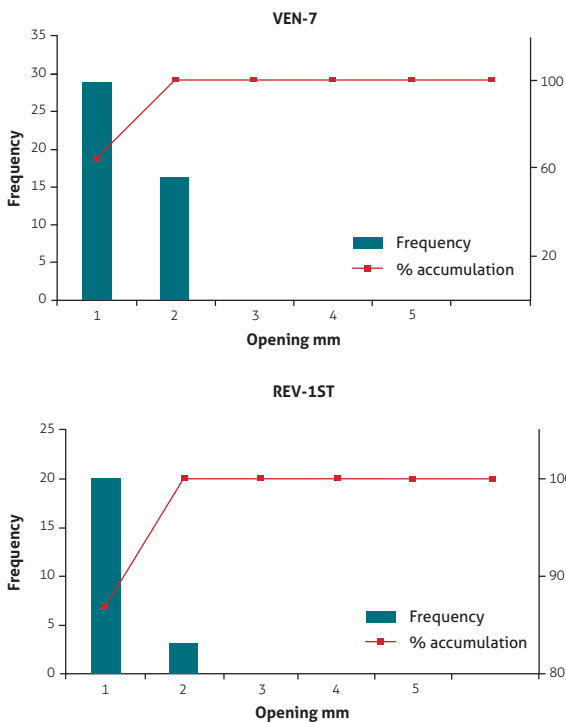


Figure 13. Examples of fracture diagrams. Left: Pozo VEN-40 Arup, microfaults 5440-6084' MD. Right: Pozo VEN-15 Arlo, conductive fractures 5496-5760' MD

The apertures of some fractures were also measured in core samples with simple techniques such as by using

gauges. Most apertures were smaller than 2 mm, and most values were approximately 1 mm or less (Figure 14).



MD	VEN-7	ARIN 3	
	#FRAC Natu	Observations	Opening mm
5321	1	Subhorizontal	2
5320	1	30°	1
5319	0		
5318	0		
5317	0		
5316	1	30°	1
5315	0		
5314	2	1. Parallel to bedding 2. 20-25°	2
5313	1	30°	1
5312	2	30°	1
5309	2	1. Parallel to bedding 2. 20-25°	2
5308	1	30°	2
5307	1	Subhorizontal	1
5306	1	Parallel to bedding	2
5305	1	30°	1
5303	3	30° Conjugated	1
5302	1	Parallel to bedding	2
5300	2	1. Parallel to bedding 2. 20-25°	1

MD	REV-1ST	ARSU 2-3	
	#FRAC Natu	Observations	Opening mm
5683	1	Subhorizontal	2
5680	1	Subhorizontal	2
5673	0	1 vein subvertical	
5668	0	1 vein subvertical	
5667	0	Carbonaceous nodule (no HC)	
5666	1	Subvertical (fault plane)	1
5665	0	Veins parallel to fractal	
5660	1	Subhorizontal close bedding	1
5659	1	Subhorizontal close bedding	1
5658	1	Subhorizontal cercar estratification	1
5656	1	Subhorizontal	1
5654	1	Subhorizontal	1
5653	1	Subhorizontal	1
5651	0	Subvertical veins in calcareous bedding 0.5'-1'	
5650	1	Subhorizontal	2
5645	1	Subhorizontal	1
5644	1	Subhorizontal, veins	1
5643	0	Conjugated veins, 30-40°	

Figure 14. Graphs of the aperture of fractures in millimeters measured in core samples. Top: VEN-7 well. Total fractures: 45; parallel to the bedding: 13 (28%). Bottom: REV-1ST well. Total fractures: 24; parallel to the bedding: 4 (17%)

In the reservoirs that, in addition to their primary characteristics, are considered naturally fractured (Henning et al., 2000), a correct 4D technical and economic evaluation of the quality and arrangement of discontinui-

ties is essential to determine their actual contribution to improving the petrophysical properties of such reservoirs (Figure 15).

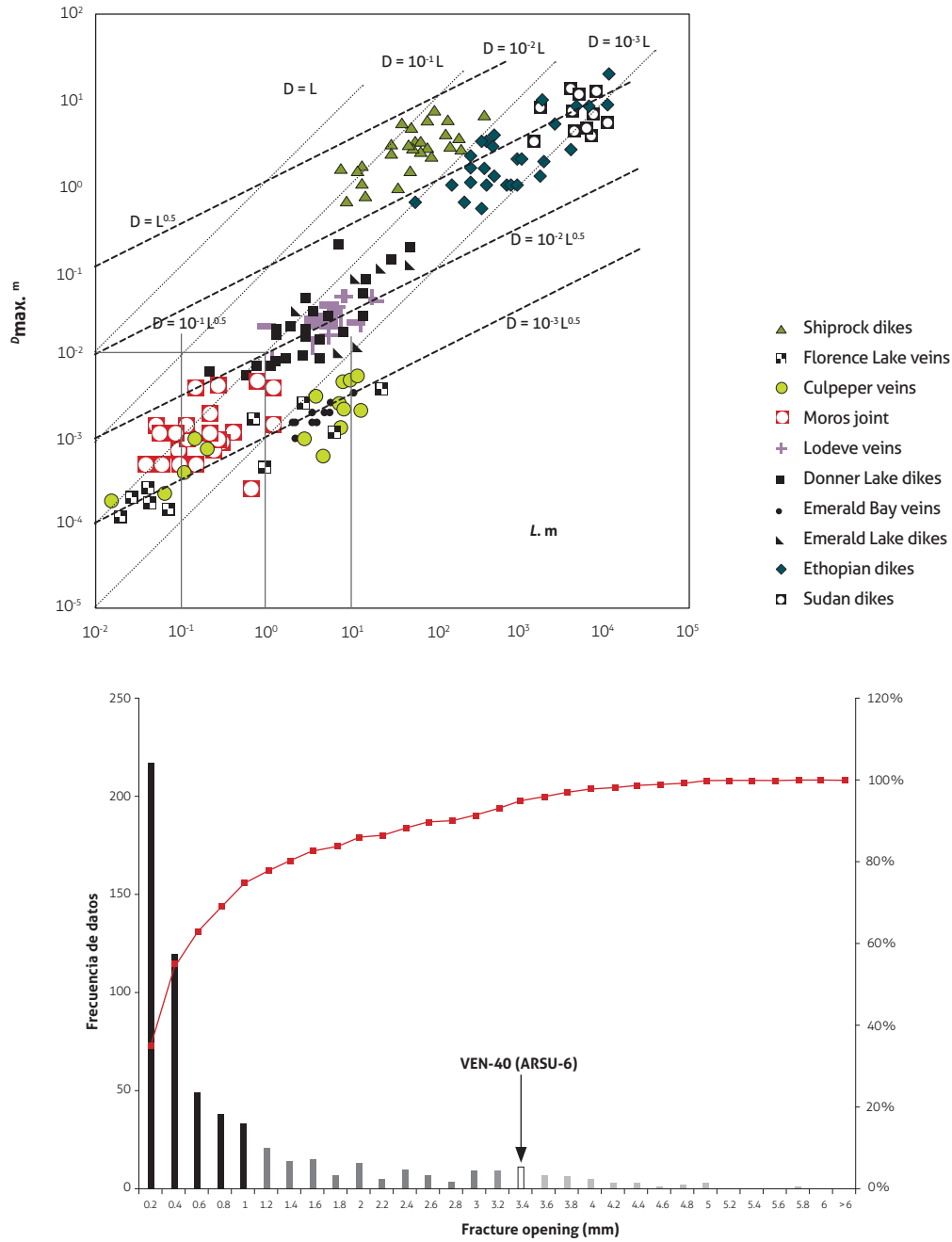


Figure 15. Fracture aperture in millimeters from BHI records

Left: compilation of D/L ratios of ten fracture aperture sets. Fracture length vs. fracture aperture as a function of n- 0.5 exponents. The dashed black lines represent square root functions. Gray dashed lines are linear functions (retrieved from Klimczak et al., 2009). *Right:* histogram of fracture aperture vs. frequency

The relationships between the permeabilities and porosities of hydrocarbon-producing horizons of the Guadalupe Formation in some wells derived from the South and North Matachines Fields show fairly regular behaviors, albeit with different dispersions, most likely due to the direction of the intersecting boreholes (Figure 16).

The relationships between porosity and horizontal permeability in core samples corresponding to the levels of the Arup and Arlo horizons in the VEN-1, VEN-17, REV-1ST, REV-2ST, and REV-6 wells of North and South Matachines clearly show that bedding-lamination produced mechanical boundaries that increased permeability (Figure 17).

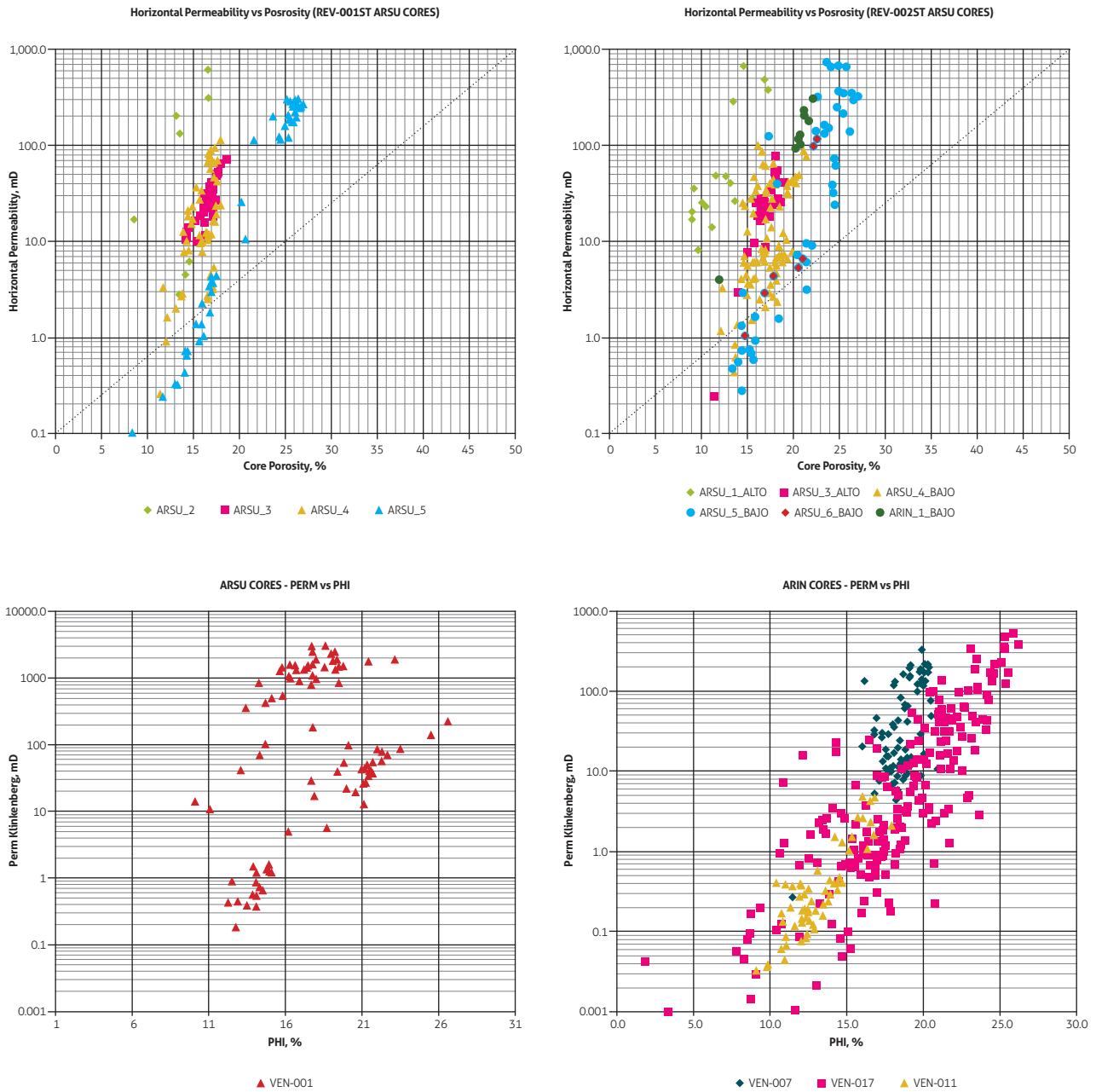


Figure 16. Graphs of relationships between porosity and permeability in core samples from wells
 Top: Arup horizons in the South Matachines Field. Bottom: Arup and Arlo horizons in the North Matachines Field

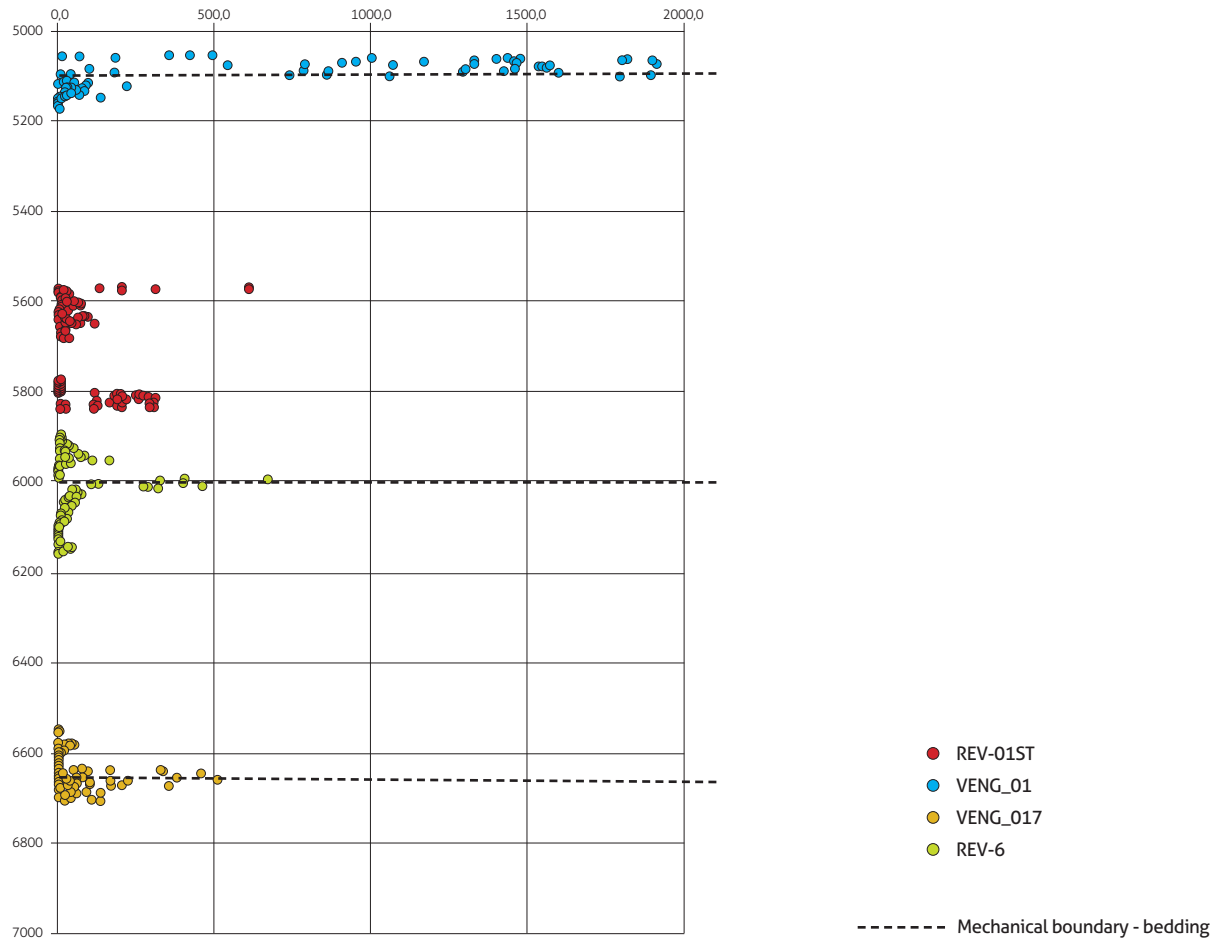


Figure 17. Relationship between core depth and permeability of hydrocarbon-producing horizons, wherein permeability increases at the mechanical boundaries between layers

Permeability was compared between vertical and horizontal wells, considering permeability data in hydrocarbon-producing horizons within stratigraphic units expressing mechanically active boundaries, showing that permeability is higher in horizontal wells than in vertical wells (Figure 18).

The greater permeability of horizontal wells should have been generated by their location in the top hinge section of the main structure of the field (Figure 12), which in turn has higher flexural slip folding and therefore higher permeability in the stratigraphic mechanical boundaries. For this reason, horizontal wells parallel to the bedding in the hinge areas are more likely to inter-

sect dilating sectors with better porosity and secondary permeability characteristics. Furthermore, when they are located in the top sections of the hinges, the locally more extensional conditions favor their development.

Based on the morphostructural features identified in the surface and subsoil data, the Matachines fields shows a multiphase evolution, which may have been controlled, at least partly, by pre-existing Paleozoic anisotropies. The new structural interpretation on the geologic time scale shows a main fault in the WNW–ESE direction in the North Matachines field, which is consistent with the fracture data from the BHI analyses (Figure 19).

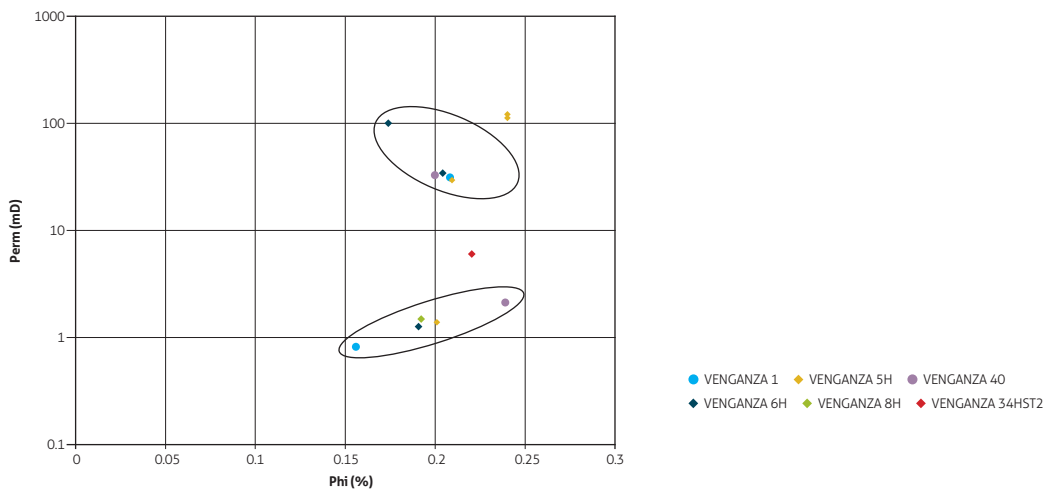


Figure 18. Comparative graph of the permeabilities of the same sands or stratigraphic units (mechanical boundaries) of vertical and horizontal wells

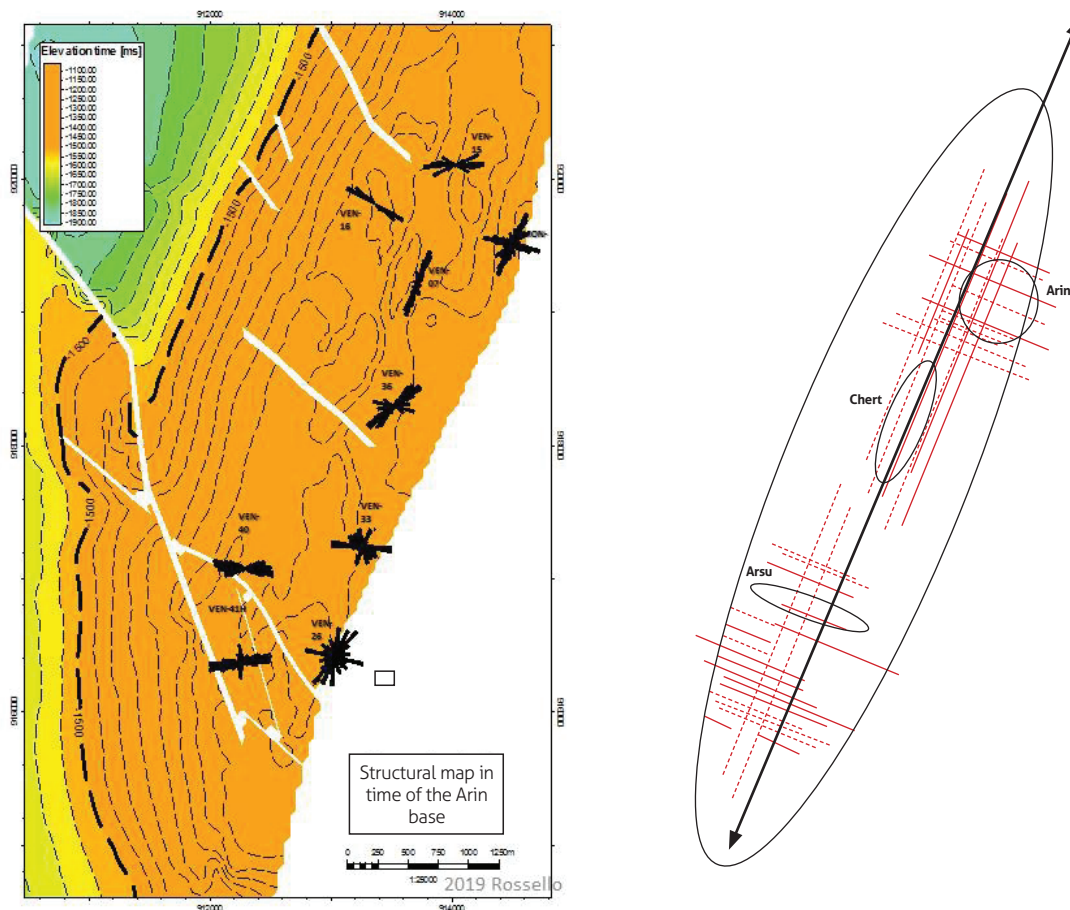


Figure 19. Plan view of the conceptual model of the permeability domains related to the interpreted fracture patterns. Areas with numerous fracture intersections highlight interconnected fracture patterns determining a likely circular drainage. Areas where fractures lack intersections show a more elliptical drainage pattern because they run parallel to the fractures

Accordingly, many commonly used methods for studying wells from core samples or images (Nelson, 1985; Nelson and Serra, 1995; Rider, 1986; Ortega and Marret, 2000; Laongsakul and Dürrast, 2011) identify different types of discordant fractures, but the bedding surfaces are evaluated separately, which does not statistically con-

sider the petrophysical effects that contribute to porosity and permeability (Figure 20). Discontinuities due to bedding planes are highly important because they control the distribution of fluids running parallel to the main axis of folding.

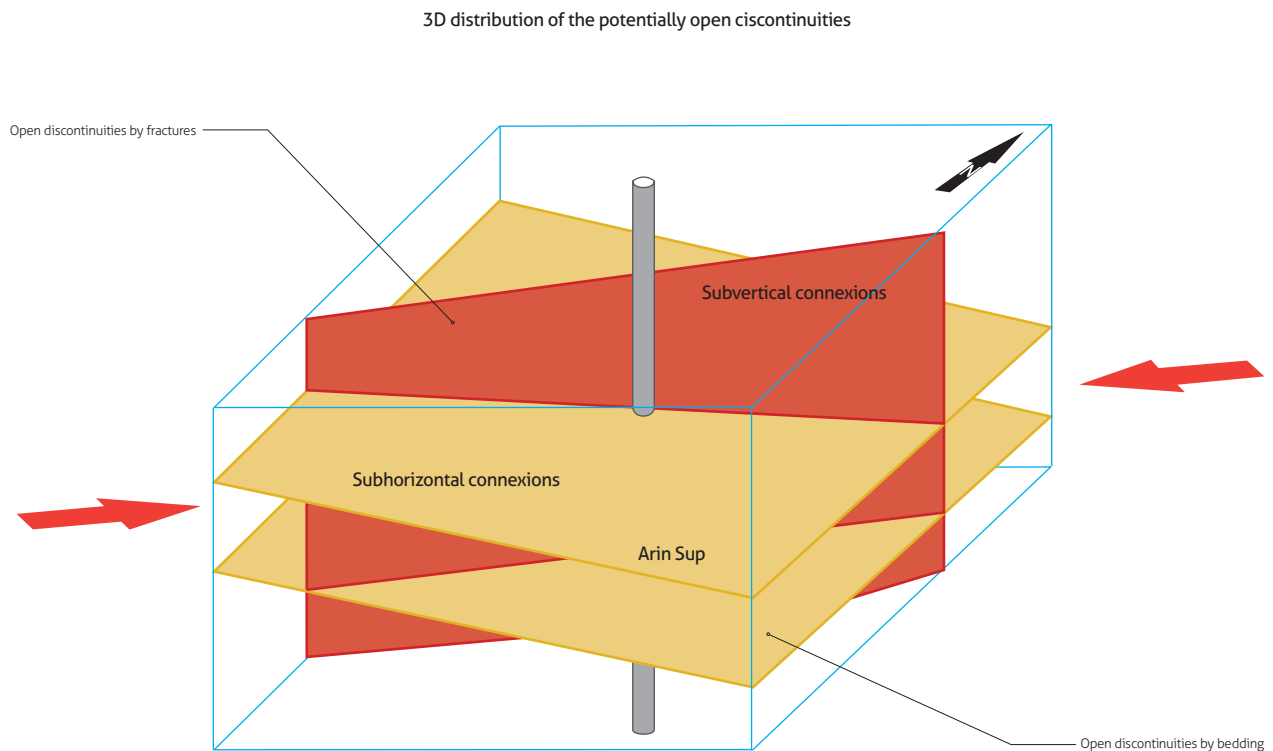


Figure 20. Idealized diagram of spatial relationships of subvertical fracture and bedding planes that contribute to fluid circulation in the Upper Arlo horizons of the Guadalupe Formation

7. DISCUSSION

The action of a compressive stress field is responsible for the structural style of this basin, characterized by the successive action of the Incaic and Quechua phases between the Eocene and recent times, which started with the reactivation of the pre-existing normal fault planes during the distensive tectonics between the late Paleozoic and the early Cretaceous (Figure 21).

The tensional state produced by successive Andean tectonic phases has remained active for a long time, as shown by the differential deformation of sedimentary sequences, which was more intense in those deposited earlier because they have accumulated deformations from this stage to now (overlapping phases). Thus, these earlier (Cretaceous) horizons may exhibit a more pronounced clockwise rotation of fractures than those generated in the later (Neogene) sequences of the study area (Figure 22).

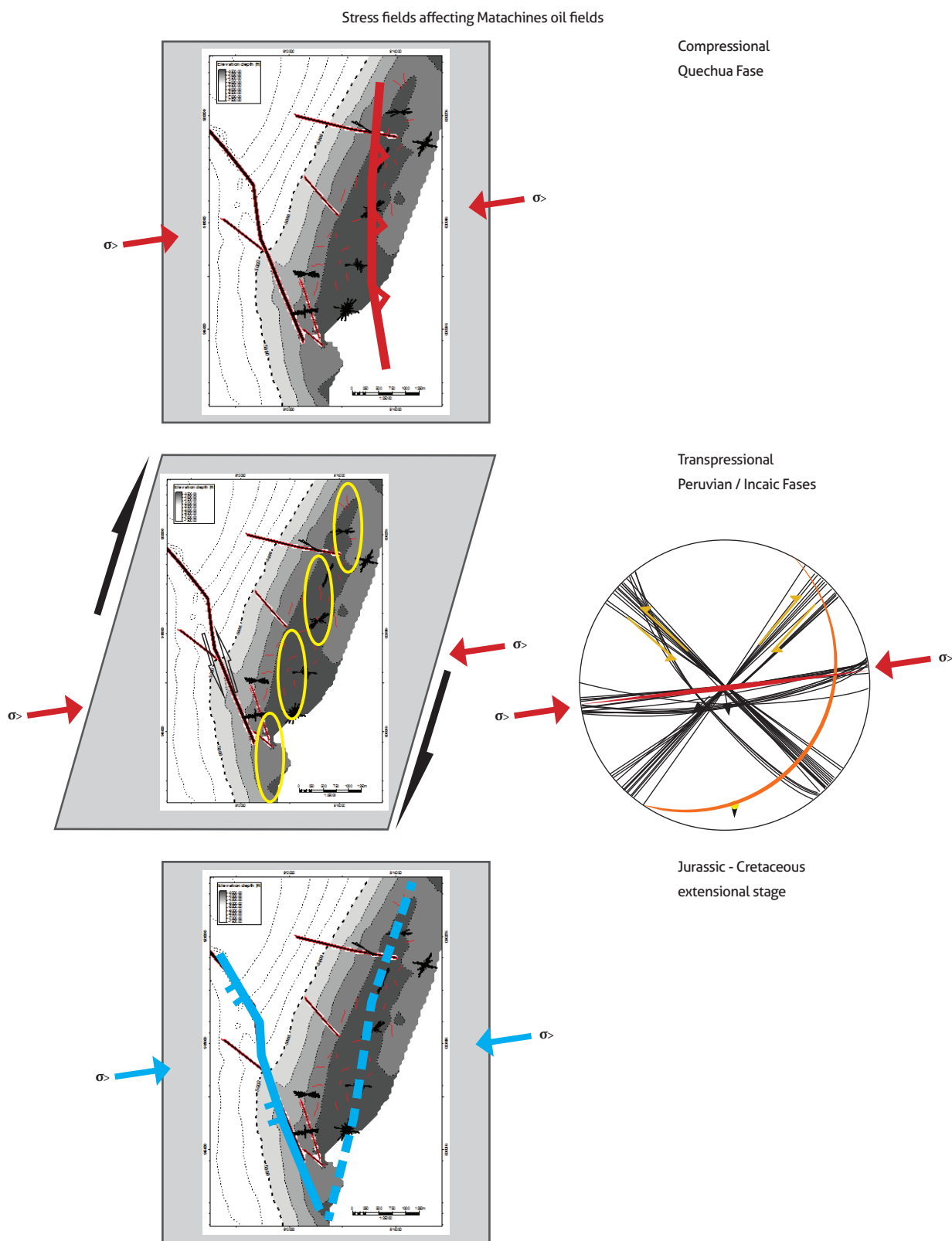


Figure 21. Evolutionary diagrams of the position of the active stress fields of the Jurassic-Cretaceous and Andean phases on the Matachines field

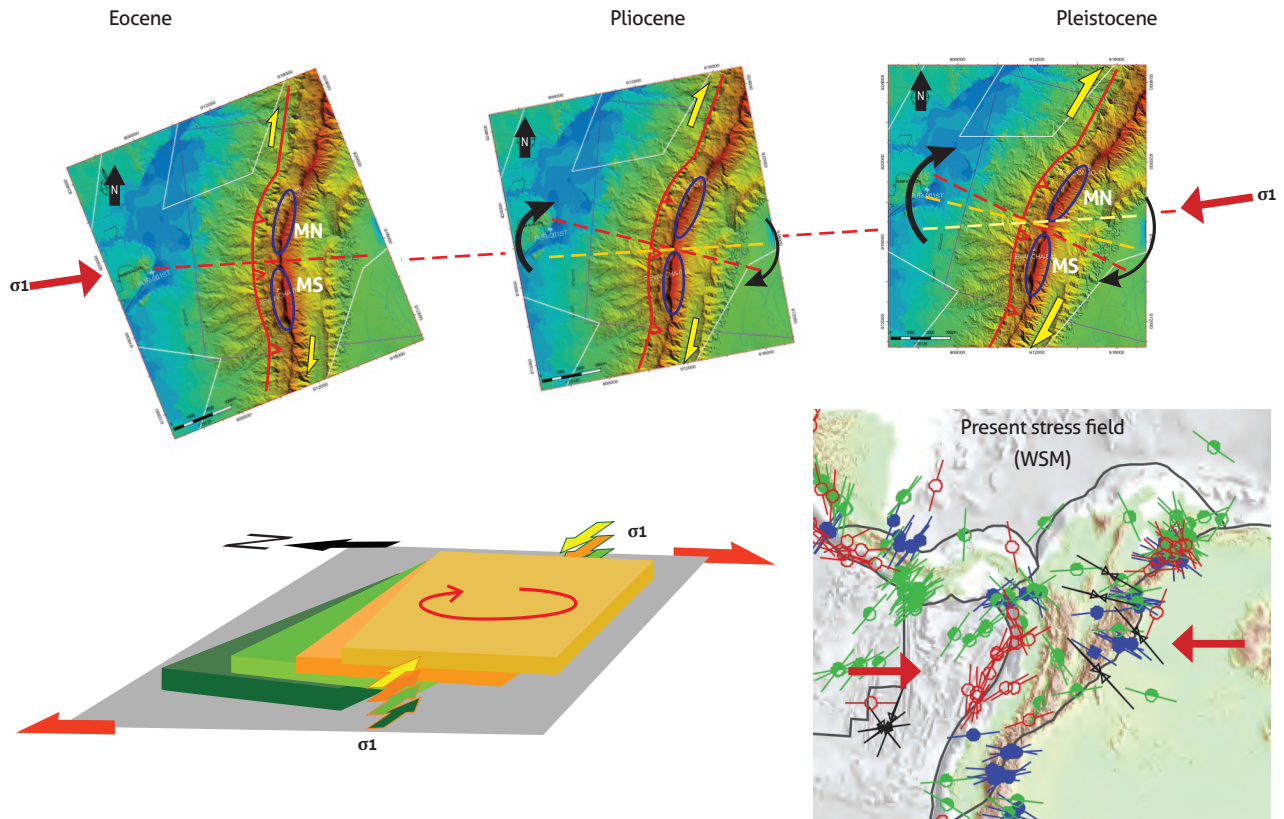


Figure 22. Evolutionary diagram of the invariable arrangement of the stress field during Andean tectonics and clockwise rotation of the study area. *Top:* three ideal states of the model with the invariant stress field (σ_1). Red, the Prado faulting; dashed yellow line, the transfer zone that separates the Matachines fields, which are indicated by blue ellipses (MN and MS). Yellow arrows indicate dextral strike-slip components. *Bottom left:* rotational model whose older levels accumulate greater rotation. *Bottom right:* focal mechanism data (circles) retrieved from the World Stress Map indicating an approximately WSW–ENE direction of convergence (red arrows)

Thus, a simplified scheme highlights discontinuous tectonic features with warped surfaces, suggesting an increase in (clockwise or counterclockwise) rotation with depth (Figure 23). These sigmoidal warps, regardless of possible stress changes due to localized and variable effective geologic overpressures, would be based on the fact that sequences deposited earlier accumulate more rotational deformation than sequences deposited later within an invariant stress field in space throughout a contemporary span with all sequences involved (Rossello, 2018).

Due to the structuring characteristics of the Matachines field, the boreholes are concentrated in the NNW–SSE quadrant (subvertical fractures), mostly with a slightly plunging direction due to bedding surfaces, so it is more likely for there to be a higher number of potentially open fractures per linear meter of their trajectory in the

reservoir horizons of the Guadalupe Formation (Figure 24).

CONCLUSIONS

In reservoirs with primary sedimentological characteristics that are considered naturally fractured, a correct 4D technical and economic evaluation of the quality and arrangement of discontinuities should include the effect of the bedding. Many commonly used methods for studying hydraulic fracturing from core samples or images identify bedding surfaces. However, the bedding surfaces, when evaluated separately, are not sufficiently accounted for in the petrophysical considerations that contribute to porosity and permeability.

The seismic data collected in a WorkStation and mounted on the Petrel platform make it possible to spa-

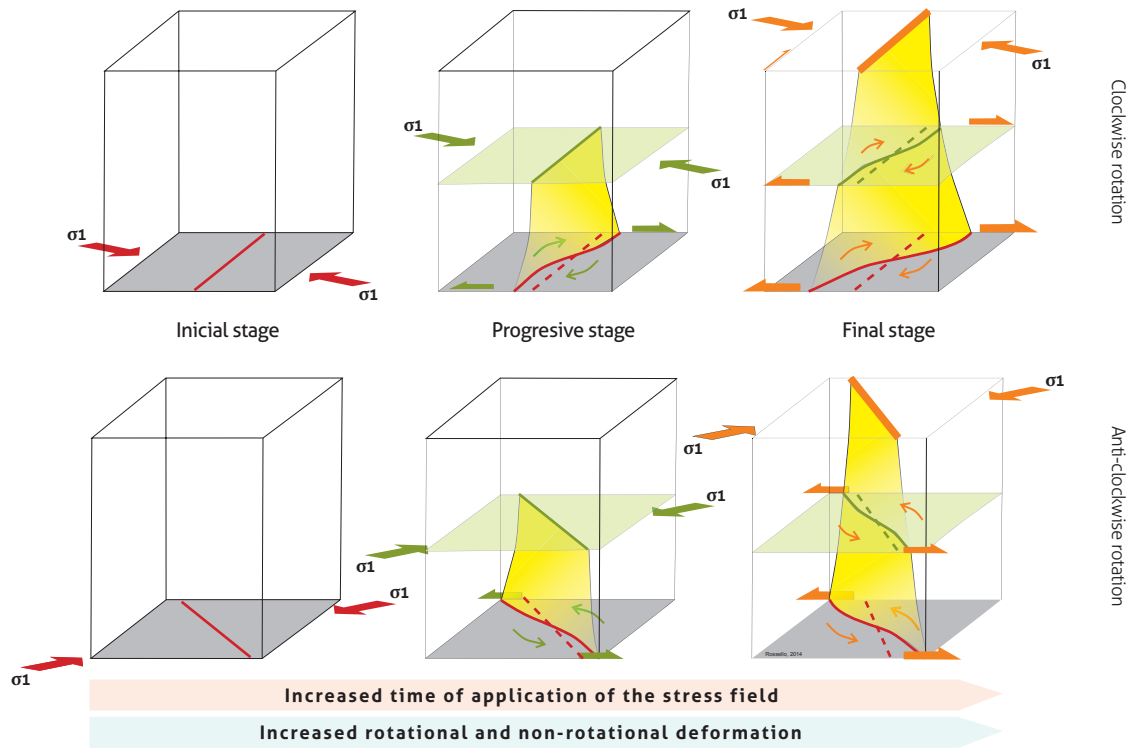


Figure 23. Evolutionary diagram of fault rotation as a function of depth within a long-term stress field. Earlier sequences exhibit greater rotations than later sequences, as a function of the time they remain in a syntectonic stress field (retrieved from Rossello, 2018)

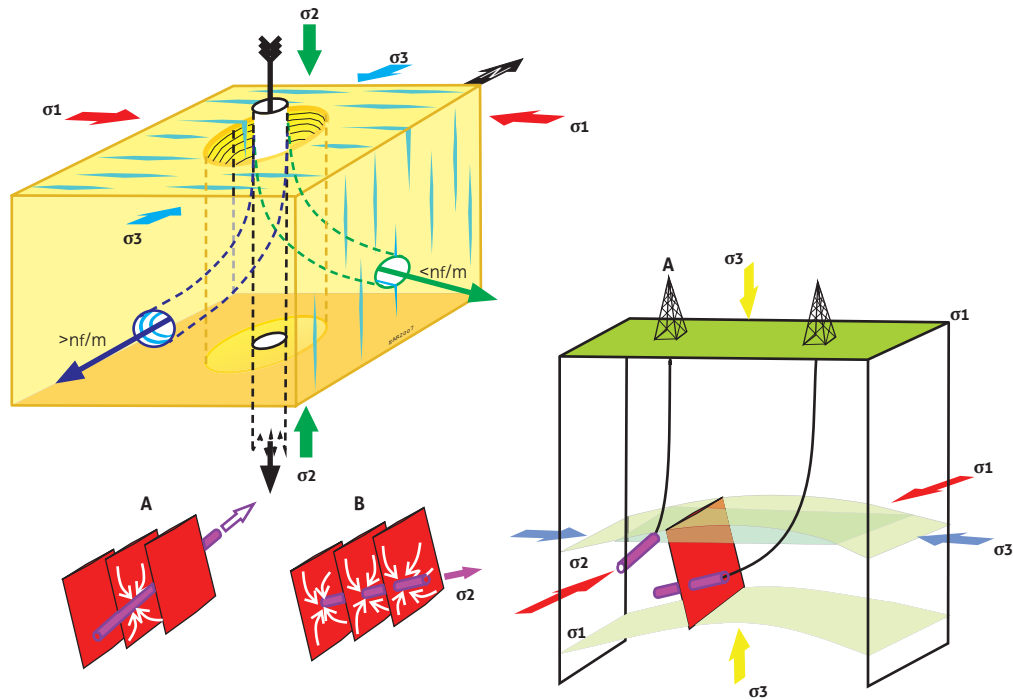


Figure 24. Schematic diagram of the preferential direction of a borehole with the highest likelihood of finding potentially open fractures along the borehole. The direction perpendicular to the dilating fractures corresponds to the minimum principal stress σ_3 (retrieved from Rossello, 2018)

tiotemporally characterize, with a mechanical criterion of deformation, a series of pre- and postdiscordance structures preceding the Honda Group. This tectonic context favors the development of deformations that tend to express clockwise rotations as a function of the time in this stress field. Thus, early generated structures have a higher clockwise rotation rate than structures generated later.

The NW–SE transverse zone that separates the two Matachines fields is considered a transfer zone resulting from an initially normal fault subjected to a sinistral strike-slip reactivation that has been timely and efficient to compartmentalize the oil system.

All the available tectosedimentary data on the Matachines field and on the spatial characteristics of the hydraulic fracturing assessed in the wells show that the evolution of the oil system is based on the following processes: 1) extensional tectonics, as shown by the normal growth of the faults that accommodated the deposition of the Lower Cretaceous sequences; 2) the transpressional deformation that occurred during the late Cretaceous, which reactivated pre-existing normal faults; 3) burial due to deposition and erosion from the Tertiary; and 4) the structuring that occurred during the Miocene, which caused the uplift of the area, and the resulting erosion and reactivation of previous structures. Therefore, the most important and efficient traps, in terms of timeliness, are those that formed during the late Cretaceous, before the maturation of the hydrocarbons.

Bedding surfaces are mechanically active planes that have enhanced the flexural slip produced by the folding of multilithological sequences. In the Matachines field, bedding improves the petrophysical characteristics of its reservoirs by incorporating a significant number of discontinuities, thereby complementing fluid connectivity from subhorizontal positions through planes of subvertical fractures generated by the horizontal compressional stresses preferentially arranged in the ENE–WSW direction. In particular, these effects are magnified on the western flank of the anticline structure and near its top hinge, resulting in their strong effect on the connectivity of production wells from their subhorizontal positions, with the action of subvertical fracture planes generated by the compressional efforts preferentially arranged in the ENE–WSW direction.

ACKNOWLEDGMENTS

The colleagues at Hocol Petroleum Limited are thanked for their valuable discussions throughout this study, which helped us understand the technical and regional aspects of the Matachines field. The meticulous editorial work and thoughtful comments and suggestions from the anonymous referees greatly improved the clarity of this work.

REFERENCES

- Acosta, J., Lonergan, L., & Coward, M. P. (2004). Oblique transpression in the western thrust front of the Colombian Eastern Cordillera. *Journal of South American Earth Sciences*, 17 (3), 181-194. <https://doi.org/10.1016/j.jsames.2004.06.002>
- Aguilera, R. (2001). *Naturally fractured reservoirs* (2nd ed.). Tulsa: Penn Well Publishing Company.
- Aguilera, R., & Aguilera, R. (2004). A triple porosity model for petrophysical analysis of naturally fractured reservoirs. *Petrophysics*, 45 (2), 157-166.
- Anderson, T. A. (1972). Paleogene non-marine Guanday Group, Neiva Basin, Colombia, and regional development of the Colombian Andes. *GSA Bulletin*, 83 (8), 2423-2438. [https://doi.org/10.1130/0016-7606\(1972\)83\[2423:PNGGNB\]2.0.CO;2](https://doi.org/10.1130/0016-7606(1972)83[2423:PNGGNB]2.0.CO;2)
- Barrero, D., Pardo, A., Vargas, C. A., & Martínez J. F. (2007). *Colombian sedimentary basins: Nomenclature, boundaries and petroleum geology, a new proposal*. Bogotá: Agencia Nacional de Hidrocarburos y B&M Exploration Ltda.
- Bayona, G. A., García, D. F., & Pabón, G. M. (1994). La Formación Saldaña: producto de la actividad de estratovolcanes continentales en un dominio de retro-arco. In F. Etayo Serna (ed.), *Estudios geológicos del Valle Superior del Magdalena* (cap. I, pp. 1-121). Bogotá: Universidad Nacional de Colombia.
- Beltrán, N., & Gallo, J. (1979). The geology of the Neiva Sub-Basin, Upper Magdalena Basin, southern portion. In *ACGGP, Geological field trips Colombia, 1959-1978* (pp. 253-275). Bogotá: Geotec.
- Blanco, M. A., & De Freitas, M. G. (2003). Geología estructural de la zona de Yaguará-Palermo, piedemonte

- de la cordillera Central, valle superior del Magdalena, Colombia. In *Memorias del 8.º Simposio Bolivariano de Exploración Petrolera en las Cuencas Subandinas* (Cartagena) (t. I, pp. 21-33).
- Bratton, T., Viet Canh, D., Van Que, N., Duc, N. V., Gillespie, P., Hunt, D., Li, B., Marcinew, R., Ray, S., Montaron, B., Nelson, R., Schoderbek, D., & Sonneland, L. (2006). The nature of naturally fractured reservoirs. *Oilfield Review*, 18, Summer, 4-23.
- Buitrago, J. (1994). Petroleum systems of the Neiva area, Upper Magdalena Valley, Colombia. In L. Magoon, & W. G. Dow (eds.), *The petroleum system: From source to trap* (pp. 483-497). Tulsa: American Association of Petroleum Geologists.
- Butler, K., & Schamel, S. (1988). Structure along the eastern margin of the Central Cordillera, Upper Magdalena Valley, Colombia. *Journal of South American Earth Sciences*, 1 (1), 109-120. [https://doi.org/10.1016/0895-9811\(88\)90019-3](https://doi.org/10.1016/0895-9811(88)90019-3)
- Campbell, C. J., & Burgl, H. (1965). Section through the Eastern Cordillera of Colombia, South America. *GSA Bulletin*, 76 (5), 567-590. [https://doi.org/10.1130/0016-7606\(1965\)76\[567:STTECO\]2.0.CO;2](https://doi.org/10.1130/0016-7606(1965)76[567:STTECO]2.0.CO;2)
- Cobbold, P. R., Rossello, E. A., Roperch, P., Arriagada, C., Gómez, L. A., & Lima, C. (2007). Distribution, timing, and causes of Andean deformation across South America. In A. C. Ries, R. W. H. Butler, & R. H. Graham (eds.), *Deformation of the continental crust: The legacy of Mike Coward* (pp. 321-343). Special Publications, 272. Geological Society of London,
- Cooper, M. A., Addison, F. T., Álvarez, R., Coral, M., Graham, R. H., Hayward, A. B., Howe, S., Martínez, J., Naar, J., Peñas, R., Pulham, A. J., & Taboada, A. (1995). Basin development and tectonic history of the Llanos Basin, Eastern Cordillera and Magdalena Valley, Colombia. *American Association of Petroleum Geologists, Bulletin*, 79 (10), 1421-1443. <https://doi.org/10.1306/7834D9F4-1721-11D7-8645000102C1865D>
- Corrigan, H. T. (1967). The geology of the Upper Magdalena Basin. In ACGGP, *Geological fieldtrips, Colombia 1959-1978* (pp. 221-251). Reprinted by Geotec, 1992, Bogotá.
- Cossio, U., Rodríguez, G., & Rodríguez, M. (1995). *Geología de la plancha 283, Purificación. Escala 1:100.000*. Bogotá: Ingeominas.
- De Freitas, M. G. (2001). Exploring for subthrust traps in a transpressional setting: A review of unsuccessful results and strategies for improvement in the Upper Magdalena Valley of Colombia. AAPG Hedberg Conference (Mendoza), extended abstract.
- De Freitas, M. G., & Vallejo, J. (2000). Condicionantes estructurales y estratigráficos en el yacimiento terciario de río Ceibas, cuenca alto Magdalena, Colombia. In *Memorias del 7.º Simposio Bolivariano de Exploración Petrolera en Cuencas Subandinas* (Caracas) (pp. 207-217).
- De Freitas, M. G., Vidal, G., & Mantilla, M. (2006). Structural evolution and hydrocarbon entrapment in the Balcon field area, Upper Magdalena Valley, Colombia. In *Actas del 9.º Simposio Bolivariano de Exploración en Cuencas Subandinas* (Bogotá) (pp. 253-275). Asociación Colombiana de Geólogos y Geofísicos del Petróleo.
- Duarte, E., Cardona, A., Lopera, S., Valencia, V., & Estupiñán, H. (2018). Provenance and diagenesis from two stratigraphic sections of the Lower Cretaceous Caballos Formation in the Upper Magdalena Valley: Geological and reservoir quality implications. *Ciencia, Tecnología y Futuro*, 8 (1), 5-29.
- Ekstrom, M. P., Dahan, C. A., Chen, M. Y., Lloyd, P. M., & Rossi, D. J. (1987). Formation imaging with microelectrical scanning arrays. *The Log Analyst*, 28, 294-306.
- Fisher, N. I., Lewis, T. L., & Embleton, B. J. (1987). *Statistical analysis of spherical data*. Cambridge: Cambridge University Press.
- George, R. P., Pindell, J. L., & Cristancho, J. (1997). Eocene paleostructure of Colombia and implications for history of generation and migration of hydrocarbons. Exploración petrolera en las cuencas subandinas. In *Memorias del 6.º Simposio Bolivariano* (Bogotá) (t. II, pp. 133-140). Asociación Colombiana de Geólogos and Geofísicos del Petróleo.
- Gómez, E., Jordan, T. E., Allmendinger, R. W., Hegarty, K., Kelley, S., & Heizler, M. (2003). Controls on architecture of the Late Cretaceous to Cenozoic Southern Middle Magdalena Valley Basin, Co-

- lombia. *GSA Bulletin*, 115 (2), 131-147. [https://doi.org/10.1130/0016-7606\(2003\)115<0131:COAOT-L>2.0.CO;2](https://doi.org/10.1130/0016-7606(2003)115<0131:COAOT-L>2.0.CO;2)
- Guerrero, J. (2002). Proposal on the classification of systems tracts: Application to the allostratigraphy and sequence stratigraphy of the Cretaceous Colombian Basin. Part 2: Barremian to Maastrichtian. *Geología Colombiana*, 27, 27-49.
- Hennings, P., Olson, J., & Thomson, L. (2000). Combining outcrop data and three dimensional structural models to characterize fracture reservoirs: An example from Wyoming. *AAPG Bulletin*, 84 (6), 830-849. <https://doi.org/10.1306/A967340A-1738-11D7-8645000102C1865D>
- Higuera, D. A. (2012). *Modelo petrofísico integrado del Grupo Guadalupe, aplicado al campo Matachín Norte* (M.Sc. thesis). Universidad Nacional de Colombia.
- Irving, E. M. (1975). Structural evolution of the northernmost Andes, Colombia. *U. S. Geological Survey Professional Paper*, 846, 1-47. <https://doi.org/10.3133/pp846>
- Jaimés, E., & De Freitas, M. G. (2006). An Albian-Cenomanian unconformity in the Northern Andes: Evidence and tectonic significance. *Journal of South American Earth Sciences*, 21 (4), 466-492. <https://doi.org/10.1016/j.jsames.2006.07.011>
- Jamison, W. (1997). Quantitative evaluation of fractures on Monkshood Anticline, a detachment fold in the foothills of Western Canada. *AAPG Bulletin*, 81 (7), 830-849. <https://doi.org/10.1306/522B-49FB-1727-11D7-8645000102C1865D>
- Klimczak, C., Schultz, R. A., Parashar, R., & Reeves, D. M. (2009). Cubic law with aperture-length correlation: Implications for network scale fluid flow. *Hydrogeology Journal*, 18 (4), 851-862. <https://doi.org/10.1007/s10040-009-0572-6>
- Kroonenberg, S. B., & Diederix, H. (1982). Geology of the uppermost Magdalena Valley. In Geotec, *Geological field trips: Colombia, 1980-1989* (pp. 73-89). Bogotá: Asociación Colombiana de Geólogos and Geofísicos del Petróleo.
- Kubik, W., & Lowry, P. (1993). Fracture identification and characterization using Cores, FMS, CAST, and Borehole Camera: Devonian shale, Pike County, Kentucky. Paper SPE 25897 presented at the 1993 SPE Rocky Mountain Regional/Low Permeability Reservoirs Symposium, Denver, CO, 12-14 April.
- Laongsakul, P., & Dürrast, H. (2011). Characterization of reservoir fractures using conventional geophysical logging. *Songklanakarin Journal of Science and Technology*, 33 (2), 237-246.
- Mojica, J., & Franco, R. (1990). Estructura y evolución tectónica del valle medio y superior del Magdalena, Colombia. *Geología Colombiana*, 17, 41-64.
- Montes, C., Hatcher, R., & Restrepo, P. (2005). Tectonic reconstruction of the Northern Andean blocks: Oblique convergence and rotations derived from the kinematics of the Piedras-Girardot area, Colombia. *Tectonophysics*, (1-4), 399, 221-250. <https://doi.org/10.1016/j.tecto.2004.12.024>
- Mora, A., Mantilla, M., & De Freitas, M. G. (2010). Cretaceous paleogeography and sedimentation in the Upper Magdalena and Putumayo Basins, Southwestern Colombia. *Search and Discovery Article*, 50246.
- Nelson, R. A. (1985). *Geologic analysis of naturally fractured reservoirs*. Houston: Gulf Publishing Co.
- Nelson, R. A., & Serra, S. (1995). Vertical and lateral changes in fracture spacing in several folded carbonate sections and its relation to locating horizontal wells. *Journal of Canadian Petroleum Technology*, 34 (6), 51-56. <https://doi.org/10.2118/95-06-05>
- Ortega, O., & Marret, R. (2000). Prediction of macrofracture properties using microfracture information: Mesaverde Group Sandstones, San Juan Basin, New Mexico-Texas. *Journal of Structural Geology*, 22 (5), 571-588. [https://doi.org/10.1016/S0191-8141\(99\)00186-8](https://doi.org/10.1016/S0191-8141(99)00186-8)
- Pindell, J., & Tabbutt, K. D. (1995). Mesozoic-Cenozoic Andean paleogeography and regional controls on hydrocarbon systems. In A. J. Tankard, R. Suárez, & H. J. Welsink (eds.), *Petroleum Basins of South America* (pp. 101-128). American Association of Petroleum Geologists, Memoir 62.
- Rider, M. H. (1986). *The geological interpretation of well logs*. New York: John Wiley & Sons, Inc.
- Rossello, E. A. (2018). Interpretaciones estructurales dinámicas a partir del análisis de ovalización (break-outs) de pozos: aplicaciones a perforaciones en la Formación Vaca Muerta (cuenca neuquina, Argentina).

Revista de la Asociación Geológica Argentina, 75 (2), 252-264.

- Saavedra, J. L. (2013). *Geometría y evolución cinemática del sector que separa los campos Matachín Norte y Matachín Sur, bloque Espinal-valle superior del Magdalena, Colombia* (M.Sc. thesis). Universidad Nacional de Colombia.
- Sarmiento, L. F. (2001). *Mesozoic rifting and Cenozoic Basin inversion history of the Eastern Cordillera, Colombian Andes: Inferences from tectonic models* (Ph. D. thesis). Vrije Universiteit, Amsterdam.
- Sarmiento, L. F., & Rangel, A. (2004). Petroleum systems of the Upper Magdalena Valley, Colombia. *Marine and Petroleum Geology*, 21 (3), 373-391. <https://doi.org/10.1016/j.marpetgeo.2003.11.019>
- Schamel, S. (1991). Middle and Upper Magdalena Basins, Colombia. In K. T. Biddle (ed.), *Active margin basins* (pp. 283-301). American Association of Petroleum Geologists, Memoir, 52.
- Serra, O. (2008). *Well logging handbook*. Paris: Technip Editions.
- Toro, J., Roure, F., Bordas Le Floch, N., Le Cornec Lance S., & Sassi, W. (2004). Thermal and kinematic evolution of the Eastern Cordillera fold and thrust belt, Colombia. In R. Swennen, F. Roure, & J. W. Granath (eds.), *Deformation, fluid flow, and reservoir appraisal in foreland fold and thrust belts* (pp. 79-115). Hedberg Series, 1. American Association of Petroleum Geologists.
- Trenkamp, R., Kellogg, J. N., Freymueller, J. T., & Mora, H. P. (2002). Wide plate margin deformation, Southern Central America and Northwestern South America, CASA GPS observations. *Journal of South American Earth Sciences*, 15 (2), 157-171. [https://doi.org/10.1016/S0895-9811\(02\)00018-4](https://doi.org/10.1016/S0895-9811(02)00018-4)
- Van der Wiel, A. M. (1991). *Uplift and volcanism of the SE Colombian Andes in relation to Neogene sedimentation in the Upper Magdalena Valley* (Ph. D. thesis). University of Wageningen.
- Villamil, T., Arango, C., & Hay, W. W. (1999). Plate tectonic paleoceanographic hypothesis for Cretaceous source rocks and cherts of Northern South America. In E. Barrera, & C. C. Johnson (eds.), *Evolution of the Cretaceous ocean: climate system* (Boulder, Colorado), vol. 332. Geological Society of America. <https://doi.org/10.1130/0-8137-2332-9.191>